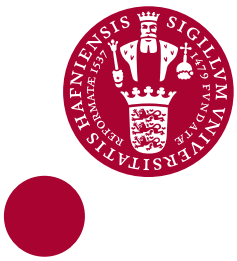

Search for direct top squark pair production in final states with two tau leptons in pp collisions at root s=8 TeV with the ATLAS detector

Aad, G.; Abbott, B.; Abdallah, J.; Abdinov, O.; Aben, R.; Abolins, M.; AbouZeid, O.S.; Abramowicz, H.; Abreu, H.; Abreu, R.; Acharya, B.S.; Aielli, G.; Ahlen, S. P.; Adomeit, S.; Adams, David L.; Dam, Mogens; Hansen, Jørn Dines; Hansen, Jørgen Beck; Xella, Stefania; Hansen, Peter Henrik; Petersen, Troels Christian; Thomsen, Lotte Ansgaard; Pingel, Almut Maria; Løvschall-Jensen, Ask Emil; Alonso Diaz, Alejandro; Monk, James William; Pedersen, Lars Egholm; Wiglesworth, Graig; Galster, Gorm Aske Gram Krohn

Published in:
European Physical Journal C

DOI:
10.1140/epjc/s10052-016-3897-z

Publication date:
2016

Document version
Publisher's PDF, also known as Version of record

Eur. Phys. J. C (2016) 76:81
DOI 10.1140/epjc/s10052-016-3897-z

THE EUROPEAN PHYSICAL JOURNAL C

Regular Article - Experimental Physics

Search for direct top squark pair production in final states with two tau leptons in pp collisions at $\sqrt{s} = 8$ TeV with the ATLAS detector

ATLAS Collaboration[⋆]

CERN, 1211 Geneva 23, Switzerland

Received: 18 September 2015 / Accepted: 14 January 2016 / Published online: 16 February 2016

Abstract A search for direct pair production of the supersymmetric partner of the top quark, decaying via a scalar tau to a nearly massless gravitino, has been performed using 20 fb^{-1} of proton–proton collision data at $\sqrt{s} = 8$ TeV. The data were collected by the ATLAS experiment at the LHC in 2012. Top squark candidates are searched for in events with either two hadronically decaying tau leptons, one hadronically decaying tau and one light lepton, or two light leptons. No significant excess over the Standard Model expectation is found. Exclusion limits at 95 % confidence level are set as a function of the top squark and scalar tau masses. Depending on the scalar tau mass, ranging from the 87 GeV LEP limit to the top squark mass, lower limits between 490 and 650 GeV are placed on the top squark mass within the model considered.

Contents

1 Introduction

Additional partners of the top quark are ingredients in several models that address the hierarchy problem [1–4] of the Standard Model (SM). Supersymmetry (SUSY) [5–13] is one such model which naturally resolves the hierarchy problem with the introduction of supersymmetric partners of the known bosons and fermions. A supersymmetric partner of the top quark would stabilise the Higgs boson mass against quadratically divergent quantum corrections, provided that its mass is close to the electroweak symmetry breaking energy scale. This would make its discovery possible at the Large Hadron Collider (LHC) [14]. In a generic R-parity-conserving minimal supersymmetric extension of the SM (MSSM) [15–19], the scalar partners of right-handed and left-handed quarks, $\tilde{q}_{\mathrm{R}}$ and $\tilde{q}_{\mathrm{L}}$, can mix, as can the scalar partners of charged leptons, $\tilde{\ell}_{\mathrm{R}}$ and $\tilde{\ell}_{\mathrm{L}}$, to form two squark or two slepton mass eigenstates, respectively. The lighter of the two top squark eigenstates is denoted $\tilde{t}_1$ and is referred to as the scalar top in the following. Likewise, the lighter of the two scalar tau eigenstates is denoted $\tilde{\tau}_1$ and referred to herein as the scalar tau.

In gauge-mediated supersymmetry breaking (GMSB) models [20–25], the spin-3/2 partner of the graviton, called the gravitino $\tilde{G}$, is assumed to be the lightest supersymmetric particle. Assuming that the mass scale of the messengers responsible for the supersymmetry breaking is of the order of 10 TeV, in order to minimise fine tuning [26], the scalar top should be lighter than about 400 GeV [27]. If the scalar tau is lighter than the scalar top, and the supersymmetric partners of the gauge and Higgs bosons (charginos and neutralinos) are heavier, the dominant decay mode of the $\tilde{t}_1$ might be the three-body decay into $b\nu_\tau\tilde{\tau}_1$, where ν_τ is the tau neutrino, followed by the $\tilde{\tau}_1$ decay into a tau lepton and a gravitino. The other possible decay mode is the two-body decay into a top quark and a gravitino. The partial width of the two-body decay depends on the gravitino mass, while the partial width of the three-body decay via a virtual chargino depends on the chargino mass, as well as the chargino and scalar top mixing. For fixed scalar top and scalar tau masses either mode can dominate, and we focus in this paper on the signature result-

⋆ e-mail: atlas.publications@cern.ch

ing from the three-body decay. The two-body decay would give a signature very similar to that of the decay into a top quark and a neutralino, which has been addressed in previous searches [28–34]. In the simplest gauge-mediated models, the predicted Higgs boson mass [35] is typically lower than the measured mass [36], especially if a light scalar top is also required. However, a variety of mechanisms exist [37–41] to raise the Higgs boson mass to make it compatible with the observed value.

A lower limit of 87 GeV on the mass of the scalar tau has been set by the LEP experiments [42–46]. No limits have been published so far from hadron collider searches for the three-body decay of the scalar top into the scalar tau. Searches for scalar top pair production in proton–proton (pp) collisions, targeting the decay into charginos or neutralinos, have been performed by the ATLAS [28] and CMS [29–34] collaborations. Searches for scalar tops decaying into gravitinos, but not including the scalar tau in the decay chain, have been reported by the ATLAS [47] and CMS [48,49] collaborations.

This paper presents a dedicated search for pair production of scalar tops resulting in a final state with two tau leptons, two jets that contain a b-hadron (b-jets), and two very light gravitationally interacting particles. The decay topology of the signal process is shown in Fig. 1; the model considered is a simplified model in which all the supersymmetric particles other than the scalar top and the ones entering its decay chain are decoupled. In order to maximise the sensitivity, two distinct analyses have been performed based on the decay mode of the tau leptons in the final state: one analysis requires two hadronically decaying tau leptons (the hadron–hadron channel) and the other requires one hadronically decaying tau lepton and one tau decaying into an electron or muon, plus neutrinos (the lepton–hadron channel). In addition, the results of the search reported in Ref. [50], which is sensitive to events where both tau leptons decay leptonically (referred to as the lepton–lepton channel), are reinterpreted and limits are set on the scalar top and scalar tau masses.

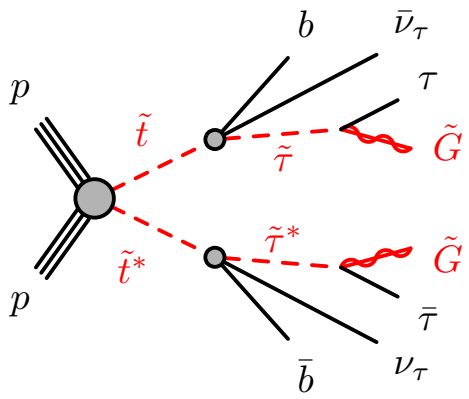

Fig. 1 Diagram showing the decay topology of the signal process

2 ATLAS detector

ATLAS [51] is a multi-purpose particle physics experiment at the LHC. The ATLAS detector[1] consists of an inner tracking detector surrounded by a superconducting solenoid, electromagnetic and hadronic calorimeters, and a muon spectrometer. The inner detector covers $|\eta| < 2.5$ and consists of a silicon pixel detector, a semiconductor microstrip detector, and a transition radiation tracker (TRT). The inner detector is surrounded by a thin superconducting solenoid providing a 2 T axial magnetic field, and allows for precision tracking of charged particles and vertex reconstruction. The calorimeter system covers the pseudorapidity range $|\eta| < 4.9$. In the region $|\eta| < 3.2$, high-granularity liquid-argon electromagnetic sampling calorimeters are used. A steel/scintillator-tile calorimeter provides energy measurements for hadrons within $|\eta| < 1.7$. The end-cap and forward regions, which cover the range $1.5 < |\eta| < 4.9$, are instrumented with liquid-argon calorimeters for electromagnetic and hadronic particles. The muon spectrometer surrounds the calorimeters and consists of three large superconducting air-core toroid magnets, each with eight coils, a system of tracking chambers (covering $|\eta| < 2.7$) and fast trigger chambers (covering $|\eta| < 2.4$).

3 Monte Carlo simulations and data samples

A number of Monte Carlo (MC) simulated event samples are used to model the signal and describe the backgrounds. For the main background components, predictions are normalised to the data in control regions (CRs) and then extrapolated to the signal regions (SRs) using simulation. All MC samples utilised in the analyses are processed using either the ATLAS detector simulation [52] based on GEANT4 [53] or a fast simulation based on a parameterisation of the performance of the ATLAS electromagnetic and hadronic calorimeters [54] and GEANT4 elsewhere. Additional pp interactions in the same (in-time) and nearby (out-of-time) bunch crossings, termed pile-up, are included in the simulation, and events are reweighted so that the distribution of the number of pile-up collisions matches that in the data.

[1] ATLAS uses a right-handed coordinate system with its origin at the nominal interaction point (IP) in the centre of the detector and the z-axis coinciding with the axis of the beam pipe. The x-axis points from the IP to the centre of the LHC ring, and the y-axis points upwards. Cylindrical coordinates (r, ϕ) are used in the transverse plane, ϕ being the azimuthal angle around the beam pipe. The pseudorapidity is defined in terms of the polar angle θ as $\eta = -\ln\tan(\theta/2)$.

The signal model considered is a supersymmetric model with the gravitino as the lightest supersymmetric particle. By construction, the scalar partner of the right-handed tau lepton and the lightest scalar top[2] are the next-to-lightest and the next-to-next-to-lightest supersymmetric particles, respectively, and different signal models are simulated by varying their masses. Pair production of the scalar top is generated using HERWIG++ 2.6.3 [55] with the parton distribution functions (PDF) set CTEQ6L1 [56]. The model requires that the scalar top decays to $b\nu_\tau\tilde{\tau}_1$ via a virtual chargino with 100 % branching ratio, while the $\tilde{\tau}_1$ decays, with a 100 % branching ratio, into a tau lepton and a gravitino. Lifetimes are assumed to be small enough (below about 1 ps) that the detector response is unaffected by the decay distance of the supersymmetric particles from the primary vertex.

Signal cross sections are calculated to next-to-leading order (NLO) in the strong coupling constant α_s, adding the resummation of soft gluon emission at next-to-leading-logarithmic accuracy (NLO+NLL) [57–59]. The nominal cross section and its uncertainty are taken from an envelope of cross-section predictions using different PDF sets and factorisation and renormalisation scales, as described in Ref. [60].

The programs used to generate signal and background events, as well as details of the cross-section calculation, PDF sets, and generator tunings, are reported in Table 1.

The data sample used in this paper was recorded between March and December 2012, with the LHC operating at a centre-of-mass energy of $\sqrt{s} = 8$ TeV. The data are collected based on the decisions of a three-level trigger system [86]. Events are selected for the electron–hadron channel if they are accepted by a single-electron trigger, and for the muon–hadron channel if accepted by a single-muon trigger. For the hadron–hadron channel, a missing transverse momentum trigger is used. The trigger efficiency reaches its maximum value for leptons with a transverse momentum (p_{T}) above 25 GeV in the lepton–hadron channels, and it exceeds 97 % for a missing transverse momentum above 150 GeV in the hadron–hadron channel. After beam, detector and data-quality requirements, the integrated luminosity of the data samples is 20.3 fb^{-1} in the electron–hadron and muon–hadron channels, and 20.1 fb^{-1} [87] in the hadron–hadron channel. The difference in integrated luminosity is due to the additional data-quality requirements related to the trigger used in the hadron–hadron channel.

[2] The mixing matrix of the simulated samples is such that the lightest scalar top eigenstate is almost a pure partner of the right-handed top quark.

Table 1 Details about the MC generation of the background and signal samples

Process	Generator	Parton shower	Cross-section normalisation	PDF set	Generator tune
$t\bar{t}$	POWHEG-BOX r2129 [61,62]	PYTHIA 6.426 [63]	NNLO+NNLL [64–69]	NLO CT10 [70]	Perugia 2011C [71]
Single-top (Wt and s-channel)	POWHEG-BOX r1556 [61,72,73]	PYTHIA 6.426	NNLO+NNLL [74]	CTEQ6L1 [56]	Perugia 2011C
Single-top (t-channel)	ACERMC 3.8 [75]	PYTHIA 6.426	NNLO+NNLL [76]	CTEQ6L1	Perugia 2011C
$t\bar{t}+W/Z$	MADGRAPH5 1.3.28 [77]	PYTHIA 6.426	NLO [78]	CTEQ6L1	AUET2 [79]
WW, WZ, ZZ	SHERPA 1.4.1 [80]	SHERPA 1.4.1	NLO [81]	NLO CT10	SHERPA default
$Z/\gamma^*(\rightarrow ee/\mu\mu)$+jets	ALPGEN 2.14 [82]	HERWIG 6.520 [83]	NNLO [84]	CTEQ6L1	AUET2
$Z/\gamma^*(\rightarrow \tau\tau)$+jets	SHERPA 1.4.1	SHERPA 1.4.1	NNLO [84]	NLO CT10	SHERPA default
$W(\rightarrow \ell\nu)$+jets, $\ell = e, \mu, \tau$	SHERPA 1.4.1	SHERPA 1.4.1	NNLO [84]	NLO CT10	SHERPA default
$\tilde{t}_1\tilde{t}_1^*$	HERWIG++ 2.6.3 [55]	HERWIG++ 2.6.3	NLO+NLL [57–59]	CTEQ6L1	UE-EE-3 [85]

4 Event reconstruction

The reconstruction and selection of final-state objects used in this analysis are discussed below.

Vertex candidates from pp interactions are reconstructed using tracks in the inner detector. To identify the hard-scattering vertex in the presence of pile-up, the vertex with the highest scalar sum of the squared transverse momentum of the associated tracks, Σp_{T}^2, is defined as the primary vertex. The primary vertex is required to have at least five associated tracks with $p_{\mathrm{T}} > 400$ MeV.

Jets are reconstructed from three-dimensional clusters of energy deposits in the calorimeters using the anti-k_t jet clustering algorithm [88] using `FastJet` [89], with a radius parameter of $R = 0.4$. The differences in the calorimeter response between electrons/photons and hadrons are taken into account by classifying each cluster as coming from a hadronic or an electromagnetic shower on the basis of its shape [90]. The energy of electromagnetic and hadronic clusters is then weighted with correction factors derived from MC simulations. The average expected contribution from pile-up, calculated as the product of the jet area and the median energy density of the event [91], is subtracted from the jet energy. A further energy and η calibration based on MC simulations and data, relating the response of the calorimeter to the true simulated jet energy [92,93], is then applied. The jets selected in the analysis are the jet candidates with $p_{\mathrm{T}} > 20$ GeV and $|\eta| < 2.5$. Events containing jets that are likely to have arisen from detector noise, beam background or cosmic rays, are removed using the procedures described in Ref. [92]. Events containing any jet failing to meet specific quality criteria described in Ref. [94] are also rejected.

Among the jets satisfying the selection criteria above, b-jet candidates are identified by a neural-network-based algorithm, which utilises the impact parameters of tracks, secondary vertex reconstruction, and the topology of b- and c-hadron decays inside a jet [95,96]. The efficiency for tagging b-jets in a MC sample of $t\bar{t}$ events using this algorithm is 70 % with rejection factors of 137 and 5 against light-quark or gluon jets, and c-quark jets, respectively. To compensate for differences between the b-tagging efficiencies and mis-tag rates in data and MC simulation, correction factors derived using $t\bar{t}$ events are applied to jets in the simulation as described in Refs. [95,96].

Electron candidates used to veto events with prompt leptons in the hadron–hadron channel search are required to have $p_{\mathrm{T}} > 10$ GeV, $|\eta| < 2.47$ and to satisfy *loose* selection criteria on electromagnetic shower shape and track quality [97]. Their longitudinal and transverse impact parameters must be within 2 and 1 mm of the primary vertex, respectively. In the lepton–hadron channel, further selections are applied. Electrons are required to satisfy the *tight* quality criteria, to have $p_{\mathrm{T}} > 25$ GeV, and to be isolated within the tracking volume. The electron identification efficiencies are of about 95, 91 and 80 % for the *loose*, *medium* and *tight* working points respectively. The electron isolation requires that the scalar sum, Σp_{T}, of the p_{T} of inner detector tracks within a cone of size $\Delta R \equiv \sqrt{(\Delta\eta)^2 + (\Delta\phi)^2} = 0.2$ around the electron candidate, is less than 10 % of the electron p_{T}. The tracks included in the scalar sum must have $p_{\mathrm{T}} > 1$ GeV, are matched to the primary vertex, and do not include the electron track.

Muon candidates are reconstructed using inner detector tracks either combined with muon spectrometer tracks or matched to muon segments [98]. They are required to have $p_{\mathrm{T}} > 10$ GeV and $|\eta| < 2.4$. Their longitudinal and transverse impact parameters must be within 1 and 0.2 mm of the primary vertex, respectively. These selections have an overall efficiency of about 99 %. Muon candidates that pass these selections are referred to as *loose* muons and are used to veto events with prompt leptons in the hadron-hadron channel. The candidates with $p_{\mathrm{T}} > 25$ GeV which fulfill the isolation requirement $\Sigma p_{\mathrm{T}} < 1.8$ GeV, i.e. with at most one additional track with $1 < p_{\mathrm{T}} < 1.8$ GeV reconstructed within a cone of size $\Delta R = 0.2$ around the muon track, are referred to as *tight* muons.

Event-level weights are applied to MC events to correct for differences between the lepton reconstruction and identification efficiencies measured in the simulation, and those measured in data.

Hadronically decaying tau lepton (τ_{had}) candidates are seeded by calorimeter jets with $p_{\mathrm{T}} > 10$ GeV. An η- and p_{T}-dependent energy scale calibration is applied to correct for the detector response and subtract energy from pile-up interactions [99]. Tau lepton candidates are identified by using two boosted decision tree (BDT) algorithms that separate them from jets and electrons [99]. Variables describing the shower shape in the calorimeters and information from the tracking system are used to separate the collimated τ_{had} decay products from the generally broader jets resulting from quark and gluon hadronisation. Variables such as the number of tracks or the fraction of the total tau energy contained in a cone of size $\Delta R = 0.1$ centred on the tau candidate provide strong discriminating power. To distinguish taus from electrons, the most discriminating characteristics are the transition radiation emitted by electrons in the TRT and the longer and wider shower generated by a hadronically decaying tau in the calorimeter compared with that produced by an electron. In addition to the two BDT selection criteria, a muon veto is applied. Hadronically decaying tau lepton candidates are required to have $p_{\mathrm{T}} > 20$ GeV, $|\eta| < 2.47$, and exactly one or three associated inner detector tracks (referred to as 1-prong and 3-prong candidates, respectively). The tau candidate is assigned an electric charge equal to the sum of the charges of the associated tracks, and this is required to be either +1 or −1. Three working points (*loose*, *medium*, and

Table 2 Sequence of the overlap removal algorithm. Here, ℓ refers to electrons and muons

Condition	Discarded object
$\Delta R(\text{jet, electron}) < 0.2$	Jet
$\Delta R(\tau_{\text{had}}, \ell) < 0.2$	τ_{had}
$\Delta R(\text{jet}, \ell) < 0.4$	ℓ
$\Delta R(\tau_{\text{had}}, \text{jet}) < 0.2$	Jet

tight) are used for each BDT. The hadron–hadron channel uses the tight identification working point for jet rejection and the medium identification working point for electron rejection, while the lepton–hadron channel uses the medium working point for both. The loose working point has been used to cross-check the background modelling. For the jet-veto BDT, the working points correspond to a signal efficiency of 70, 60 and 40 % for 1-prong τ_{had}, and 65, 55 and 35 % for 3-prong τ_{had}, respectively. The electron-veto BDT working points have a signal efficiency of 95, 85 and 75 %, respectively. Efficiency scale factors are used to account for the mis-modelling of BDT input variables in the simulation. They are extracted by comparing efficiencies in data and simulation in a $Z \to \tau\tau$ selection, using a tag-and-probe method described in Ref. [99].

As a given final-state particle can be simultaneously reconstructed as (for example) an electron, a jet and a hadronically decaying tau lepton, an algorithm is used to resolve such ambiguities. Electrons satisfying the medium quality criteria, muons satisfying the criteria described above except that on isolation, jets and hadronically decaying tau candidates satisfying the selection criteria given above are considered by the algorithm. If two objects are close together in ΔR, one of them is discarded according to the sequence specified in Table 2. Electrons and muons close to jets, which are likely to originate from the decay of heavy-flavour hadrons, are removed from the list of leptons used in the analysis.

The missing transverse momentum vector $\mathbf{p}_{\text{T}}^{\text{miss}}$, whose magnitude is referred to as $E_{\text{T}}^{\text{miss}}$, is calculated as the negative vector sum of the transverse momenta of all reconstructed electrons, jets and muons, and calorimeter energy clusters not associated with any objects. For the $\mathbf{p}_{\text{T}}^{\text{miss}}$ computation, hadronically decaying taus are treated as jets. Clusters associated with electrons with $p_{\text{T}} > 10$ GeV, and those associated with jets with $p_{\text{T}} > 20$ GeV are calibrated with the electron and jet cluster calibrations, respectively. For jets, the calibration includes the pile-up correction described earlier while the *jet vertex fraction* (JVF) requirement is not imposed. The JVF variable is the ratio of the sum of the transverse momentum of the tracks associated with the jet and originating from the selected primary vertex to the total p_{T} sum of all tracks matched with the jet. This requirement rejects jets originating from pile-up. Clusters of energy deposits in calorimeter cells with $|\eta| < 2.5$ not associated with these objects are calibrated using both calorimeter and tracker information [100].

5 Event selection and background estimate

5.1 Hadron–hadron channel

For the hadron–hadron channel search, events in the signal region are required to have exactly two oppositely charged hadronically decaying taus satisfying the tight identification criteria, no electrons or muons, and at least two jets with a JVF larger than 0.5 or $p_{\text{T}} > 50$ GeV. One of the jets must be b-tagged. The leading jet must also satisfy $p_{\text{T}} > 40$ GeV.

The missing transverse momentum must be larger than 150 GeV. The $\Delta\phi$ separation between each of the two leading jets and the direction of the missing transverse momentum must be greater than 0.5 radian, to suppress events where large $E_{\text{T}}^{\text{miss}}$ arises from mis-measurement of jet energies. Beyond these preselection requirements, additional selections are made using transverse masses and derived variables, as explained below. These selections have been determined using MC signal and background samples to maximise the expected significance of the signal.

The transverse mass associated with two final-state objects a and b is defined as

$$m_{\text{T}}(\text{a, b}) = \sqrt{m_{\text{a}}^2 + m_{\text{b}}^2 + 2(E_{\text{T}}^{\text{a}} E_{\text{T}}^{\text{b}} - \mathbf{p}_{\text{T}}^{\mathbf{a}}.\mathbf{p}_{\text{T}}^{\mathbf{b}})}, \quad (1)$$

where m, E_{T} and $\mathbf{p}_{\text{T}}$ are the object mass, transverse energy and transverse momentum vector, respectively. Objects entering the m_{T} calculation are always assumed to be massless, unless the transverse mass is used as part of a derived variable in the lepton–hadron channel (see Sect. 5.2).

The *stransverse mass* (m_{T2}) [101,102] is computed as

$$m_{\text{T2}}(\text{a, b}) = \sqrt{\min_{\mathbf{q}_{\text{T}}^{\mathbf{a}} + \mathbf{q}_{\text{T}}^{b} = \mathbf{p}_{\text{T}}^{\text{miss}}} (\max[m_{\text{T}}^2(\mathbf{p}_{\text{T}}^{\text{a}}, \mathbf{q}_{\text{T}}^{\text{a}}), m_{\text{T}}^2(\mathbf{p}_{\text{T}}^{\text{b}}, \mathbf{q}_{\text{T}}^{\text{b}})])}, \quad (2)$$

where $\mathbf{q}_{\text{T}}^{\text{a}}$ and $\mathbf{q}_{\text{T}}^{\text{b}}$ are vectors satisfying $\mathbf{q}_{\text{T}}^{\text{a}} + \mathbf{q}_{\text{T}}^{\text{b}} = \mathbf{p}_{\text{T}}^{\text{miss}}$, and the minimum is taken over all the possible choices of $\mathbf{q}_{\text{T}}^{\text{a}}$ and $\mathbf{q}_{\text{T}}^{\text{b}}$.

The selection criteria that define the signal region for the hadron–hadron channel (SRHH) rely on the following variables:

- $m_{\text{T2}}(\tau_{\text{had}}, \tau_{\text{had}})$ is defined using the momenta of the hadronically decaying taus and the missing transverse momentum, which is assumed to result from two invisible massless particles. The $m_{\text{T2}}(\tau_{\text{had}}, \tau_{\text{had}})$ variable is bounded from above by the W boson mass for events

where the two hadronically decaying taus originate from the decay of two W bosons and all the missing transverse momentum is carried by the neutrinos from the W bosons decay, as is the case for the dominant background ($t\bar{t}$).

- $m_{\mathrm{T}}^{\mathrm{sum}}(\tau_{\mathrm{had}}, \tau_{\mathrm{had}})$ is defined as the sum of the transverse mass of each τ_{had} candidate and the missing transverse momentum

$$m_{\mathrm{T}}^{\mathrm{sum}}(\tau_{\mathrm{had}}, \tau_{\mathrm{had}}) = m_{\mathrm{T}}(\tau_{\mathrm{had1}}, p_{\mathrm{T}}^{\mathrm{miss}}) + m_{\mathrm{T}}(\tau_{\mathrm{had2}}, p_{\mathrm{T}}^{\mathrm{miss}}) \quad (3)$$

The $m_{\mathrm{T}}^{\mathrm{sum}}(\tau_{\mathrm{had}}, \tau_{\mathrm{had}})$ distribution is expected to reach higher values for the signal due to a larger number of invisible final-state particles than for the SM background processes.

For the SRHH signal region, the stransverse mass $m_{\mathrm{T2}}(\tau_{\mathrm{had1}}, \tau_{\mathrm{had2}})$ is required to be larger than 50 GeV while the $m_{\mathrm{T}}^{\mathrm{sum}}(\tau_{\mathrm{had1}}, \tau_{\mathrm{had2}})$ variable is required to be larger than 160 GeV. The signal selection efficiency, defined as the number of signal events that pass the full selection over the total number of generated events, is only weakly dependent on the scalar tau mass, while it increases from 0.02 to 0.7 % as the scalar top mass increases from 150 to 700 GeV, for a scalar tau mass of 87 GeV. The distributions of $m_{\mathrm{T2}}(\tau_{\mathrm{had1}}, \tau_{\mathrm{had2}})$ and $m_{\mathrm{T}}^{\mathrm{sum}}(\tau_{\mathrm{had1}}, \tau_{\mathrm{had2}})$ are illustrated in Fig. 2 after the preselection.

The background processes populating the SRHH selection are grouped into three categories. The first contains events with two real, hadronically decaying taus (*true* taus). It consists mainly of $t\bar{t}$ events, with smaller contributions from single-top-quark, Z+jets, diboson (WW, WZ, ZZ) and $t\bar{t}+V$ production, where $V = W, Z$. This set of backgrounds is estimated from simulation. The remaining backgrounds contain events where at least one tau candidate is an electron or a jet that passes the tau identification criteria (*fake* taus). The second category, which contains events with only one fake τ_{had}, is composed of $t\bar{t}$, single-top-quark and W+jets events. The third and smaller category corresponds to processes with two fake taus. It is mostly composed of $t\bar{t}$, $Z(\rightarrow \nu\nu)$+jets, and single-top-quark events, which are all estimated from simulation. It has been verified that these backgrounds are well modelled: in kinematic selections where $t\bar{t}$ with true taus is expected to be the dominant process, the ratio of data over the MC prediction is compatible with one within systematics uncertainties. The contribution from multi-jet events, where both tau candidates are fakes, is estimated from data using the jet smearing method described later in this section.

The single-fake τ_{had} backgrounds from top quark ($t\bar{t}$ and single-top) and W+jets events are estimated using MC simulations scaled to the observed number of data events in two dedicated control regions (CRHHTop and CRHHW-jets). These control regions require a single-muon trigger, one τ_{had} satisfying the *tight* quality criteria, and one muon with $p_{\mathrm{T}} > 25$ GeV that satisfies the *tight* quality criteria. The m_{T2} and $m_{\mathrm{T}}^{\mathrm{sum}}$ variables are then calculated using the tau and muon momenta, considering the invisible particles as massless. One muon and one τ_{had} are required in the control regions rather than two hadronically decaying taus in order to minimise signal contamination. Upper bounds are set on the m_{T2} and $m_{\mathrm{T}}^{\mathrm{sum}}$ variables, which make the contamination from the lepton–hadron signal negligible. Table 3 details the selections defining the two control regions and the signal region.

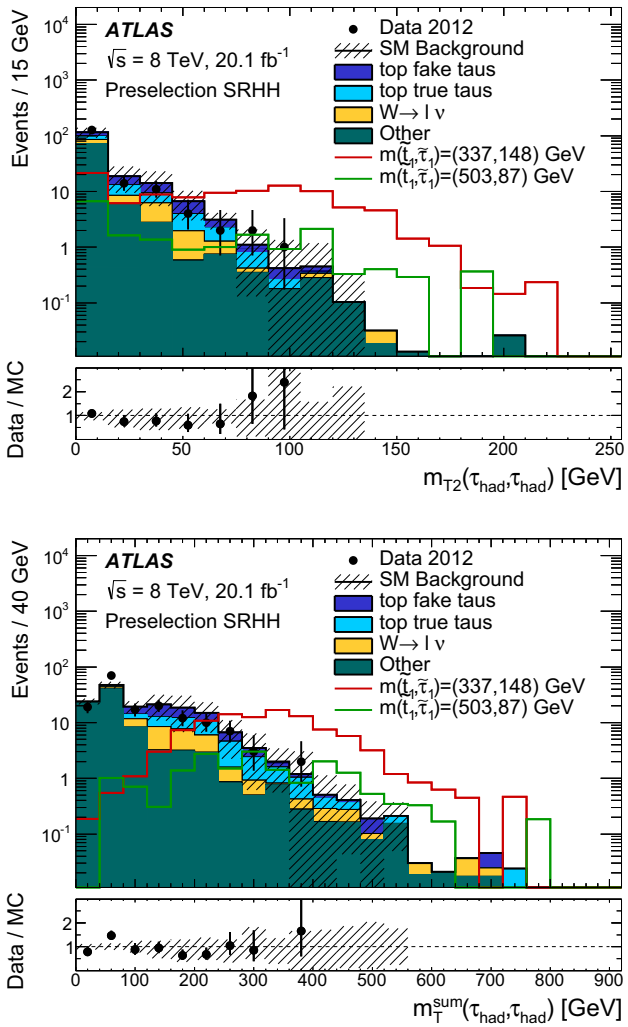

Fig. 2 *Top* Distribution of the stransverse mass constructed from the two τ_{had}, $m_{\mathrm{T2}}(\tau_{\mathrm{had}}, \tau_{\mathrm{had}})$, for events passing the hadron–hadron preselection requirements. *Bottom* Distribution of the sum of the transverse mass of each τ_{had} candidate and the missing transverse momentum, $m_{\mathrm{T}}^{\mathrm{sum}}(\tau_{\mathrm{had}}, \tau_{\mathrm{had}})$, for events passing the hadron–hadron preselection requirements. The contributions from all SM backgrounds are shown as a histogram stack; the bands represent the total uncertainty. The distributions expected for two signal models are also shown

The contributions to the background from the double-fake τ_{had} sources are smaller than 4.5 % and therefore they are estimated using simulation without normalising to data in a control region.

A simultaneous likelihood fit is performed to determine the normalisation factors of the single-fake τ_{had} backgrounds, with the number of data events in each CR as constraint, and the systematic uncertainties described in Sect. 6 included as nuisance parameters. The fit is used to predict the number of background events in the CRs and the SR. The background modelling is verified using two validation regions (VRs) by comparing the observed number of events in each VR with the number derived from the fit. The single-fake τ_{had} backgrounds from top quark and W+jets events each have a validation region, labelled VRHHTop and VRHHWjets. Like the control regions, they are defined using a muon and tau to avoid signal contamination, and the selections are summarised in Table 3. The validation regions are designed to be kinematically close to the signal region without overlapping with the control or signal regions. The composition of the control and validation regions after the fit is shown in Fig. 3. The observed and expected background yields in the VRs are in good agreement, with 50 observed events in VRHHWjets (48.5 ± 6.9 expected) and 31 observed events in VRHHTop (29.0 ± 4.1 expected). It has also been verified that a normalisation factor for the top quark background with two real τ_{had} would be compatible with one within uncertainties.

The multi-jet background is estimated from data using the jet smearing method described in Ref. [103]. A set of single-jet triggers is used to select a sample of events with at least two jets (of which at least one is required to be a b-jet), and two τ_{had} candidates. These events are required to have a low $E_{\text{T}}^{\text{miss}}$ significance,[3] to retain topologies where jets and tau candidates are well-balanced in the transverse plane and suppress processes with genuine $E_{\text{T}}^{\text{miss}}$. The energy of jets and tau candidates is then smeared within the resolution of the calorimeter, in order to simulate $E_{\text{T}}^{\text{miss}}$ arising from mis-measurements. To minimise the statistical uncertainty, no identification criteria are applied to τ_{had} candidates beyond the 1,3-track requirement, and a fake rate is used at a later stage to account for the tau identification efficiency. The pseudo-dataset obtained after smearing serves as a template for the multi-jet background. Its normalisation is derived in a multi-jet-enriched CR, labelled CRHHQCD in Table 3. To estimate the background yield in the signal region, all SRHH requirements except the tau identification are applied to the normalised background template. A weight is then applied to each event according to the probability for a jet reconstructed as a tau to satisfy the tight tau identification criteria. This fake rate is measured in data using events which fire a single-jet trigger, with at least two jets and a hadronically decaying tau candidate. It is found to be of the order of 1 % for 1-prong tau candidates and between 0.02 and 0.4 % (with a strong p_{T} dependence) for 3-prong tau candidates. The number of multi-jet events in the SR is estimated to be $0.0043 \pm 0.0007\,(\text{stat})\,^{+0.0039}_{-0.0008}\,(\text{syst})$, and is therefore neglected.

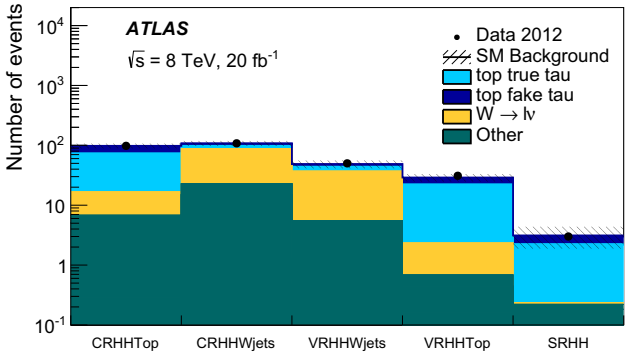

Fig. 3 Background yields and composition after the fit in the two CRs and the two VRs of the hadron–hadron channel analysis. Combined statistical and systematic uncertainties are shown as *shaded bands*. The observed number of events and the total (constrained) background are the same by construction in the CRs

5.2 Lepton–hadron channel

The search in the lepton–hadron channel requires exactly one hadronically decaying tau, exactly one isolated electron or muon with $p_{\text{T}} > 25$ GeV, and no further isolated electrons or muons with $p_{\text{T}} > 10$ GeV. The hadronically decaying tau and the lepton are required to have opposite electric charge. Each event must also contain at least two jets, where at least one of the two jets must have $p_{\text{T}} > 50$ GeV, and at least one of the two must be b-tagged.

After this common preselection, two different signal regions are defined to target signal models with a scalar top mass large or small in comparison to the top-quark mass. These are referred to as the *low-mass* (SRLM) and *high-mass* (SRHM) selections in the following, and they have been optimised with respect to the expected significance of the signal. The selections for the two signal regions are summarised in Tables 4 and 5. The low-mass selection requires a second b-jet. Three m_{T2} variables are employed in the selections, with different choices of the two visible four-momenta used in the calculation from Eq. (2):

- $m_{\text{T2}}(\ell, \tau_{\text{had}})$ uses the momenta of the light lepton and the hadronically decaying tau. The missing transverse momentum is assumed to result from two invisible mass-

[3] The $E_{\text{T}}^{\text{miss}}$ significance is defined as $E_{\text{T}}^{\text{miss}}/\sqrt{\sum_{\text{jets}} E_{\text{T}} + \sum_{\text{soft terms}} E_{\text{T}}}$ where soft terms correspond to clusters of energy deposits in the calorimeter which are not associated with any reconstructed object.

Table 3 Definition of the signal region (SRHH) for the hadron–hadron analysis. The selections of the associated control regions for $t\bar{t}$ and single-top-quark (CRHHTop) and W+jets (CRHHWjets) events with one fake hadronically decaying tau, as well as the validation regions (VRHHTop and VRHHWjets), are also shown. The ℓ entering the m_{T2} and $m_{\mathrm{T}}^{\mathrm{sum}}$ variables is either a τ_{had} (SR) or a muon (CRs and VRs)

Region	$N_{\tau_{\mathrm{had}}}$	N_{μ}	N_{jet}	$N_{b\text{-jet}}$	$E_{\mathrm{T}}^{\mathrm{miss}}$	$\Delta\phi(j_{1,2}, p_{\mathrm{T}}^{\mathrm{miss}})$	$m_{\mathrm{T2}}(\tau_{\mathrm{had}}, \ell)$	$m_{\mathrm{T}}^{\mathrm{sum}}(\tau_{\mathrm{had}}, \ell)$
SRHH	2	0	$\geq$2	$\geq$1	>150 GeV	$\geq$0.5	>50 GeV	>160 GeV
CRHHTop	1	1	$\geq$2	$\geq$1	>100 GeV	$\geq$0.5	–	[70, 120] GeV
CRHHWjets	1	1	$\geq$2	0	>100 GeV	$\geq$0.5	<40 GeV	[80, 120] GeV
VRHHTop	1	1	$\geq$2	$\geq$1	>120 GeV	$\geq$0.5	<40 GeV	[120, 140] GeV
VRHHWjets	1	1	$\geq$2	0	>120 GeV	$\geq$0.5	<40 GeV	[120, 150] GeV
CRHHQCD	$\geq$2[a]	0	$\geq$2	$\geq$1	>150 GeV	$\leq$0.5[b]	–	–

[a] For the multi-jet control region (CRHHQCD), no identification criteria are applied to tau leptons
[b] The $\Delta\phi$ requirement only applies to the sub-leading jet j_2

Table 4 Definition of the signal region SRLM used in the low-mass lepton–hadron analysis. The selections of the associated control regions for top-quark events with true taus (CRTtLM), top-quark events with fake taus (CRTfLM), and W+jets (CRWLM), and of the validation region (VRTLM) are also given

Region	$N_{b\text{-jet}}$	$H_{\mathrm{T}}/m_{\mathrm{eff}}$	$\frac{p_{\mathrm{T}}^{\ell}+p_{\mathrm{T}}^{\tau_{\mathrm{had}}}}{m_{\mathrm{eff}}}$	$m_{\mathrm{T2}}(b\ell, b)$	$m_{\mathrm{T2}}(b\ell, b\tau_{\mathrm{had}})$	$m_{\mathrm{T}}(\ell, p_{\mathrm{T}}^{\mathrm{miss}})$	m_{eff}
SRLM	$\geq$2	<0.5	>0.2	<100 GeV	<60 GeV	–	–
CRTtLM	$\geq$2	–	>0.2	<100 GeV	110–160 GeV	>100 GeV	–
CRTfLM	$\geq$2	–	>0.2	<100 GeV	110−160 GeV	<100 GeV	–
CRWLM	0	<0.5	>0.2	–	–	>40 GeV	<400 GeV
VRTLM	$\geq$2	>0.5	>0.2	<100 GeV	60−110 GeV	–	–

Table 5 Definition of the signal region SRHM used in the high-mass lepton–hadron analysis. The selections of the associated control regions for top-quark events with true taus (CRTtHM), top-quark events with fake taus (CRTfHM), and W+jets (CRWHM), and of the validation region (VRTHM) are also given

Region	$N_{b\text{-jet}}$	$E_{\mathrm{T}}^{\mathrm{miss}}$	m_{eff}	$H_{\mathrm{T}}/m_{\mathrm{eff}}$	$m_{\mathrm{T2}}(b\ell, b\tau_{\mathrm{had}})$	$m_{\mathrm{T2}}(\ell, \tau_{\mathrm{had}})$	$m_{\mathrm{T}}(\ell, p_{\mathrm{T}}^{\mathrm{miss}})$
SRHM	$\geq$1	>150 GeV	>400 GeV	<0.5	>180 GeV	>120 GeV	–
CRTtHM	$\geq$1	>150 GeV	>400 GeV	<0.5	>180 GeV	20–80 GeV	>120 GeV
CRTfHM	$\geq$1	>150 GeV	>400 GeV	<0.5	>180 GeV	20–80 GeV	<120 GeV
CRWHM	0	>150 GeV	>400 GeV	<0.5	–	20–80 GeV	40–100 GeV
VRHM	$\geq$1	<150 GeV	>400 GeV	<0.5	>180 GeV	>80 GeV	–

less particles. The $m_{\mathrm{T2}}(\ell, \tau_{\mathrm{had}})$ variable is bounded from above by the W boson mass for events where the light lepton, the hadronically decaying tau and the missing transverse momentum originate from the decay of a pair of W bosons, which is the case for most of the background ($t\bar{t}$ and Wt). The high-mass selection requires this variable to be large, because its distribution for signal models with heavy scalar taus and scalar tops peaks at higher values than for the top-quark-dominated SM background.

- $m_{\mathrm{T2}}(b\ell, b\tau_{\mathrm{had}})$ is calculated using the two jets with the highest b-tagging weight. One of them is paired with the light lepton and the other with the τ_{had}. The four-momentum vectors of the two resulting particle pairs are then used in the m_{T2} algorithm. The missing transverse momentum is assumed to be carried by two invisible massless particles. For $t\bar{t}$ events where the jet and the lepton belong to the decay of the same top quark, this variable is bounded from above by the top-quark mass. Similarly, for signal events, the upper bound on this variable is the scalar top mass. A maximum-value cut is therefore used in the low-mass selection and a minimum-value cut in the high-mass selection. The calculation of the variable requires the resolution of a two-fold ambiguity in the pairing of the jets and the leptons. Only the pairings for which $m(b\ell)$ and $m(b\tau_{\mathrm{had}})$ are both smaller than m_t are considered.[4] If exactly one pairing satisfies the condition, that pairing is used in the m_{T2} calculation. If both pair-

[4] For top-quark pair production events where the lepton and the jet belong to the decay of the same top quark, the invariant mass has an upper bound at $\sqrt{m_t^2 - m_W^2}$, approximately 152 GeV. The algorithm tries to select pairs that satisfy this condition, loosened to account for the detector resolution.

ings satisfy the condition, m_{T2} is calculated for both pairings and the smaller value is taken. If no pairing satisfies the condition, the event is considered to have passed the $m_{\mathrm{T2}}(b\ell, b\tau_{\mathrm{had}})$ selection for the high-mass signal region and to have failed it for the low-mass signal region.

- $m_{\mathrm{T2}}(b\ell, b)$ is only used for the low-mass selection. The system of one of the b-jets and the light lepton is considered as the first visible four-momentum. Only pairings for which $m(b\ell) < m_t$ are considered. If neither pairing satisfies the condition, the event is discarded, while if both pairings do, the pairing which yields the smaller value of $m_{\mathrm{T2}}(b\ell, b)$ is used. The invisible particle associated with this system is assumed to be massless. The other b-jet is the second visible system used in the m_{T2} calculation, and the mass of the associated invisible particle is set to the W boson mass, as the algorithm targets $t\bar{t}$ events where one lepton from a W boson decay is not detected or identified. For the dominant top-quark background, the $m_{\mathrm{T2}}(b\ell, b)$ variable is bounded from above by the top-quark mass. This variable has a softer distribution for low-mass signal events than the background, and a maximum-value cut of 100 GeV is applied.

The distributions for $m_{\mathrm{T2}}(b\ell, b\tau_{\mathrm{had}})$ and $m_{\mathrm{T2}}(\ell, \tau_{\mathrm{had}})$ are illustrated in Fig. 4 after the preselection, showing the separation between two signal models and the SM background. The $m_{\mathrm{T2}}(b\ell, b\tau_{\mathrm{had}})$ variable is used to distinguish the scalar top signal from the dominant top-quark backgrounds for both the low-mass and high-mass selections.

Another variable used in the selections is the ratio of the scalar sum of the transverse momenta of the two leading jets (H_{T}) to the effective mass, $m_{\mathrm{eff}} = E_{\mathrm{T}}^{\mathrm{miss}} + H_{\mathrm{T}} + p_{\mathrm{T}}^{\ell} + p_{\mathrm{T}}^{\tau_{\mathrm{had}}}$, where p_{T}^{ℓ} and $p_{\mathrm{T}}^{\tau_{\mathrm{had}}}$ are the transverse momenta of the lepton and the hadronically decaying tau, respectively. This ratio, $H_{\mathrm{T}}/m_{\mathrm{eff}}$, tends to be smaller for signal events because of the high number of invisible particles in the final state, and it is required to be less than 0.5. The high-mass selection also requires the missing transverse momentum to be larger than 150 GeV and m_{eff} to be larger than 400 GeV because the decay products of a high-mass scalar top would have large momenta. The low-mass selection requires $(p_{\mathrm{T}}^{\ell} + p_{\mathrm{T}}^{\tau_{\mathrm{had}}})/m_{\mathrm{eff}} > 0.2$ because the difference between the masses of the scalar top and scalar tau is relatively small in comparison to the difference between the masses of the top quark and the W boson. Finally, the $m_{\mathrm{T}}(\ell, p_{\mathrm{T}}^{\mathrm{miss}})$ variable is used to distinguish events with real tau leptons from events with fake tau leptons in the dominant top-quark background, and to distinguish multi-jet events from W+jets events. The definitions of the low-mass and high-mass SRs are summarised in Tables 4 and 5, respectively.

The signal selection efficiency of the low-mass selection is between 0.008 and 0.01 % for the models with a scalar top mass between 150 and 200 GeV, which is the target of this selection. The signal efficiency of the high-mass selection increases with the scalar top mass. For a fixed scalar top mass, it increases with the scalar tau mass as the $m_{\mathrm{T2}}(\ell, \tau_{\mathrm{had}})$ selection becomes more efficient, up to the region with $m(\tilde{t}_1) - m(\tilde{\tau}) < 50$ GeV where the b-jets become too soft to be efficiently detected. Outside this region, which is better targeted by the lepton–lepton channel, the efficiency of the high-mass selection varies between 0.0007 and 1 % for a scalar top mass between 200 and 700 GeV.

In the lepton–hadron channel, the ratio of real to fake hadronically decaying tau events depends on the background

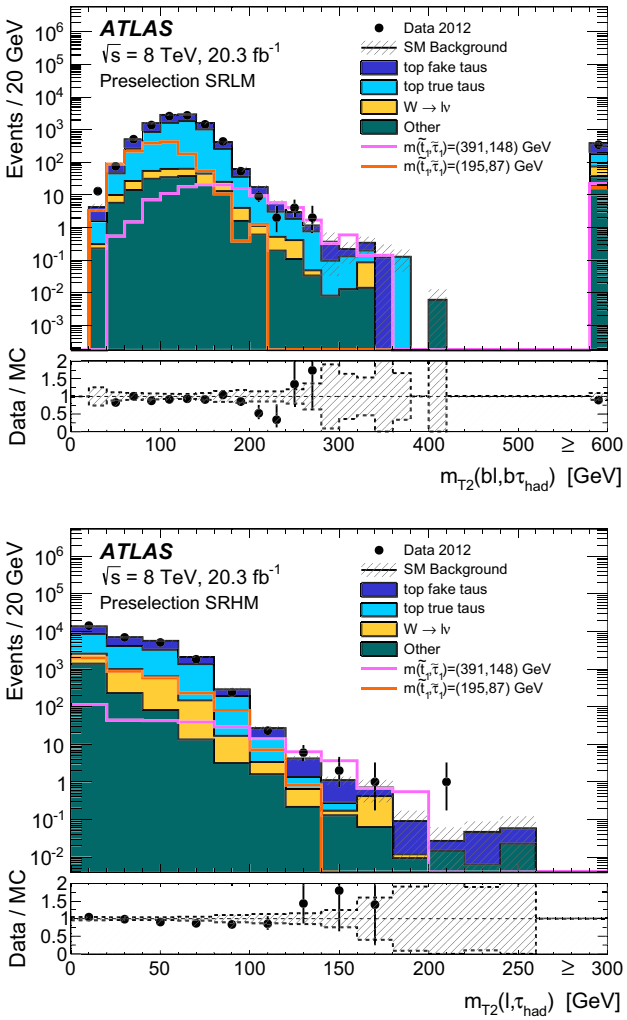

Fig. 4 *Top* Distribution of the stransverse mass constructed from the b-jet plus lepton and b-jet plus τ_{had}, $m_{\mathrm{T2}}(b\ell, b\tau_{\mathrm{had}})$, for events passing the lepton–hadron preselection requirements with the additional requirement of a second b-tagged jet. *Bottom* Distribution of the stransverse mass constructed from the momenta of the light lepton and the hadronically decaying tau, $m_{\mathrm{T2}}(\ell, \tau_{\mathrm{had}})$, for events passing the lepton–hadron preselection requirements. The contributions from all SM backgrounds are shown as a *histogram stack*; the bands represent the total uncertainty. The overflow bin in the $m_{\mathrm{T2}}(b\ell, b\tau_{\mathrm{had}})$ plot is filled with the events that have no $(b\ell, b\tau_{\mathrm{had}})$ pairing satisfying $m(b\ell) < m_t$ and $m(b\tau_{\mathrm{had}}) < m_t$. The distributions expected for two signal models are also shown

process. In W+jets events, the light lepton is always a real lepton from the W decay, due to the high reconstruction efficiency and purity of final-state electrons and muons, while the τ_{had} is faked by a recoiling hadronic object. In $t\bar{t}$ and Wt events, the light lepton originates from the decay of one of the W bosons while the hadronically decaying tau candidate can be either a real or a fake tau. These processes (W+jets, $t\bar{t}$, and Wt) are the main background sources and are estimated by MC simulation scaled to the observed data in three CRs for each SR. The CRs are enriched in either W+jets, top-quark events with true hadronically decaying taus, or top-quark events with fake hadronically decaying taus (where the top-quark events include both single and pair production), and are used to derive normalisation factors for these three categories of background. For the low-mass selection SRLM, the true- and fake-tau top-quark backgrounds are controlled by CRTtLM and CRTfLM, while CRWLM controls the W+jets background. For the high-mass selection SRHM, the three control regions CRTtHM, CRTfHM and CRWHM are used to normalise the true- and fake-tau top-quark backgrounds and the W+jets background. The CRs are defined in Table 4 for the low-mass selection and in Table 5 for the high-mass selection. The minor contribution from other background processes is estimated from simulation.

A simultaneous likelihood fit is performed to obtain the three normalisation factors for each SR, using the observed number of data events in each CR as constraints, and with the systematic uncertainty sources (described in Sect. 6) treated as nuisance parameters. The fit is used to predict the number of background events in the CRs and the SR. The validity of the background modelling is verified by using a validation region for each SR and comparing the observed number of events with the prediction from the fit. For the low-mass selection, the validation region VRLM is defined in Table 4, while the validation region VRHM is defined in Table 5 for the high-mass selection.

The background composition and the observed number of events in each CR as well as in the VR and SR are shown in Fig. 5 for the low-mass selection and in Fig. 6 for the high-mass selection. The observed and expected background yields in the VRs are in good agreement, with 386 observed events for the low-mass selection (351 ± 84 expected) and 17 observed events in the high-mass selection (22 ± 5 expected). The expected background yields and observed number of events in the SRs are reported in Sect. 7.

The background estimate with fake hadronically decaying taus (either from top-quark or W+jets events) is validated using an alternative method. The observed rate of events with a light lepton and a τ_{had} with the same electric charge is scaled by the expected ratio of opposite-sign (OS) to same-sign (SS) events for the fake τ_{had} backgrounds, which is estimated from MC simulation. Too few SS events are observed for the SRHM selection to make a meaningful prediction, so the method is only viable for the looser SRLM selection, for which it predicts 12 ± 6 events with fake hadronically decaying taus, in agreement within uncertainties with the sum of W+jets and top-quark events with fake hadronically decaying taus obtained from the fit, which is 12 ± 5 events.

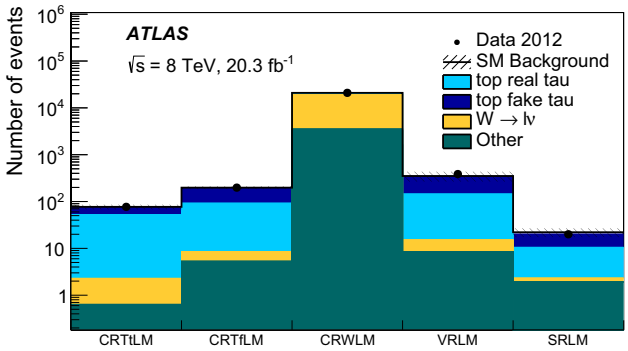

Fig. 5 Background yields and composition after the fit for the three CRs and the VR in the lepton–hadron channel low-mass selection. Combined statistical and systematic uncertainties are shown as *shaded bands*. The observed number of events and the total (constrained) background are the same by construction in the CRs

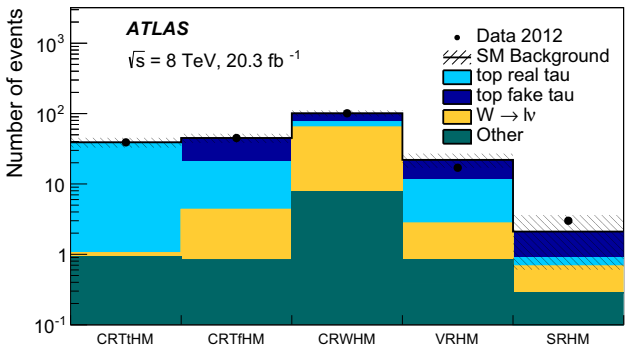

Fig. 6 Background yields and composition after the fit for the three CRs and the VR in the lepton–hadron channel high-mass selection. Combined statistical and systematic uncertainties are shown as *shaded bands*. The observed number of events and the total (constrained) background are the same by construction in the CRs

6 Systematic uncertainties

Various sources of systematic uncertainty affecting the predicted background yields in the signal regions are considered. The uncertainties are either computed directly in the SR when backgrounds are estimated from simulation, or propagated through the fit for backgrounds that are normalised in CRs.

The dominant detector-related systematic uncertainties considered in these analyses are the jet energy scale and resolution [92], the τ_{had} energy scale and BDT identification efficiency [99], and the b-tagging efficiency [95,96]. The energy scale and resolution of clusters in the calorimeter not associated with electrons, muons or jets, which affect the miss-

Table 6 Summary of background estimates and the associated total uncertainties.The size of each systematic uncertainty is quoted as a relative uncertainty on the total background. A dash indicates a negligible contribution to the uncertainty. The individual uncertainties can be correlated, and thus do not necessarily sum in quadrature to the total relative uncertainty

	SRHH	SRLM	SRHM
Background events	3.1 ± 1.2	22.1 ± 4.7	2.1 ± 1.5
Uncertainty breakdown [%]			
Jet energy scale and resolution	17	13	2
Tau energy scale	9	4	3
Cluster energy scale and resolution	1	2	4
b-tagging	2	4	2
Top-quark theory uncertainty	37	11	64
W+jets theory and normalisation	–	1	19
Simulation statistics	20	6	21
Top normalisation	18	6	20

Table 7 Observed number of events and background fit results for the hadron–hadron SR and the two lepton–hadron SRs. Combined statistical and systematic uncertainties are given. The uncertainties between the different background components can be correlated, so they do not necessarily sum to the total background uncertainty. A dash indicates a negligible background contribution. The nominal expectations from MC simulation are given for comparison in the lower part of the table

Channel	SRHH	SRLM	SRHM
Observed events	3	20	3
Total (constrained) background events	3.1 ± 1.2	22.1 ± 4.7	2.1 ± 1.5
Top with only true tau(s)	2.0 ± 1.1	8.2 ± 3.9	$0.2^{+0.3}_{-0.2}$
Top with at least one fake tau	0.9 ± 0.5	9.8 ± 4.5	$1.2^{+1.4}_{-1.2}$
W+jets	$0.01^{+0.02}_{-0.01}$	2.2 ± 0.6	0.4 ± 0.4
Z/γ^*+jets	$0.04^{+0.15}_{-0.04}$	1.9 ± 1.1	–
$t\bar{t} + V$	0.04 ± 0.02	–	0.3 ± 0.1
Diboson	0.14 ± 0.02	–	–
Expected background events before the fit	3.7	25.8	2.2
Top with only true tau(s)	2.0	11.5	0.18
Top with at least one fake tau	1.4	10.1	1.1
W+jets	0.01	2.4	0.65
Z/γ^*+jets	0.04	1.9	–
$t\bar{t} + V$	0.04	–	0.27
Diboson	0.14	–	–

Table 8 Left to right: Total constrained background yields, number of observed events, 95 % CL observed (expected) upper limits on the number of BSM events, $S^{95}_{\text{obs.(exp.)}}$, and the visible cross section, $\langle \mathcal{A}\epsilon\sigma \rangle^{95}_{\text{obs.(exp.)}}$

Signal region	Background	Observation	$S^{95}_{\text{obs.(exp.)}}$	$\langle \mathcal{A}\epsilon\sigma \rangle^{95}_{\text{obs.(exp.)}}$ [fb]
SRHH	3.1 ± 1.2	3	5.5 ($5.5^{+2.1}_{-1.3}$)	0.27 ($0.27^{+0.11}_{-0.06}$)
SRLM	22.1 ± 4.7	20	12.4 ($13.2^{+4.9}_{-3.5}$)	0.61 ($0.65^{+0.24}_{-0.17}$)
SRHM	2.1 ± 1.5	3	6.4 ($5.2^{+2.6}_{-0.9}$)	0.31 ($0.26^{+0.13}_{-0.04}$)

ing transverse momentum calculation, are also a source of systematic uncertainty. In all cases, the difference in the predicted background or signal between the nominal MC simulation and that obtained after applying each systematic variation is used to determine the systematic uncertainty on the background or signal estimate. Parts of the systematic uncertainties cancel when a background is estimated from a control region, but they do not cancel for processes normalised to their theoretical cross section. The remaining detector-related systematic uncertainties, such as those on lepton reconstruc-

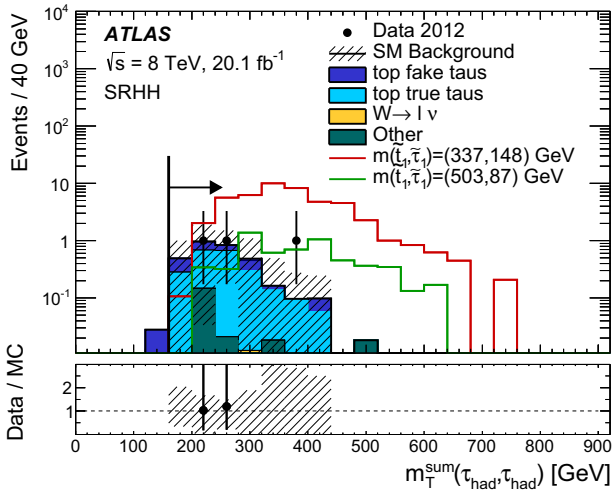

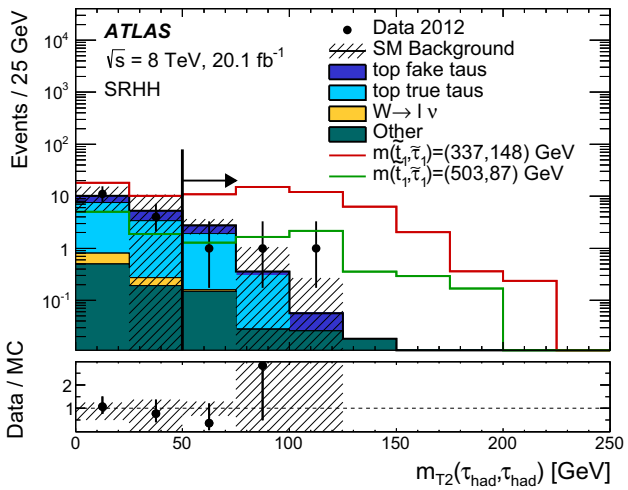

Fig. 7 *Top* Distribution of $m_{\mathrm{T}}^{\mathrm{sum}}(\tau_{\mathrm{had}}, \tau_{\mathrm{had}})$ for the events passing all the hadron–hadron signal region requirements, except that on $m_{\mathrm{T}}^{\mathrm{sum}}(\tau_{\mathrm{had}}, \tau_{\mathrm{had}})$. *Bottom* Distribution of $m_{\mathrm{T2}}(\tau_{\mathrm{had}}, \tau_{\mathrm{had}})$ for the events passing all the hadron–hadron signal region requirements, except that on $m_{\mathrm{T2}}(\tau_{\mathrm{had}}, \tau_{\mathrm{had}})$. The contributions from all SM backgrounds are shown as a histogram stack; the bands represent the total uncertainty. The background yields have been rescaled by the post-fit normalisation factors. The *arrows mark* the cut values used to define the SRs. The distributions expected for two signal models are also shown

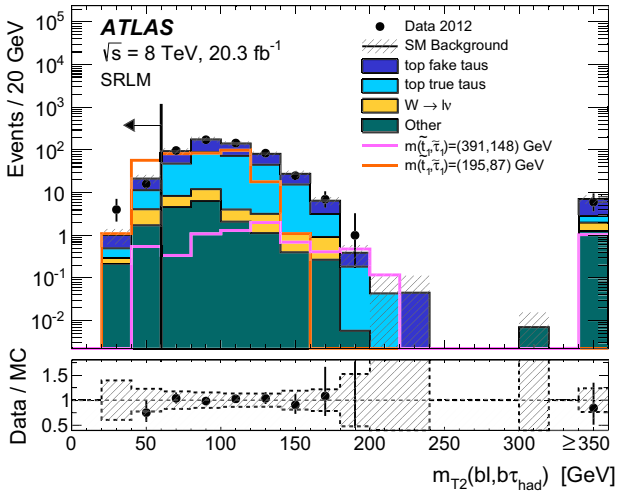

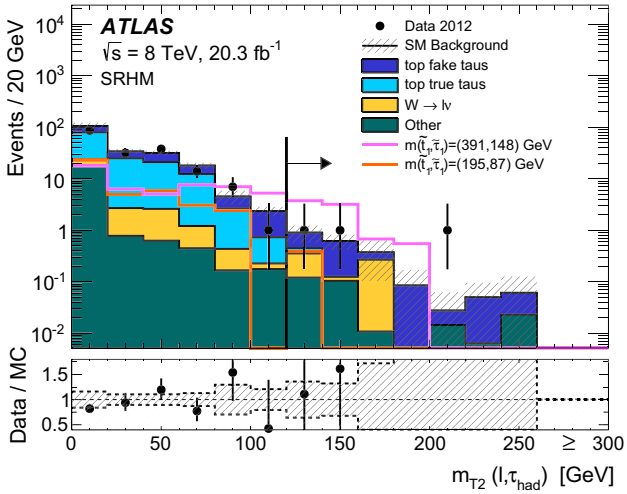

Fig. 8 *Top* Distribution of $m_{\mathrm{T2}}(b\ell, b\tau_{\mathrm{had}})$ for events passing all the lepton–hadron LM signal region requirements, except that on $m_{\mathrm{T2}}(b\ell, b\tau_{\mathrm{had}})$. *Bottom* Distribution of $m_{\mathrm{T2}}(\ell, \tau_{\mathrm{had}})$ for events passing all the lepton–hadron HM signal region requirements, except that on $m_{\mathrm{T2}}(\ell, \tau_{\mathrm{had}})$. The contributions from all SM backgrounds are shown as a *histogram stack*; the bands represent the total uncertainty. The background yields have been rescaled by the post-fit normalisation factors. The *arrows mark* the cut values used to define the SRs. The overflow bin in the $m_{\mathrm{T2}}(b\ell, b\tau_{\mathrm{had}})$ plot is filled with the events that have for both pairings of $m(b\ell)$ and $m(b\tau_{\mathrm{had}})$ at least one invariant mass larger than m_t. The distributions expected for two signal models are also shown

tion efficiency and on the modelling of the trigger, are of the order of a few percent. A 2.8 % uncertainty on the luminosity determination was measured using techniques similar to that of Ref. [87], and it is included for the normalisation of all signal and background MC samples. The signal uncertainties are between 10 and 15 % for models close to the observed exclusion contour.

Various theoretical uncertainties are considered for the modelling of the major SM backgrounds. In the case of top-quark contributions, the predictions of POWHEG-BOX are compared with those of MC@NLO-4.06 to estimate the uncertainty due to the choice of generator. The difference in the yields obtained from POWHEG-BOX interfaced to PYTHIA and POWHEG-BOX interfaced to HERWIG is taken as the systematic uncertainty due to parton shower modelling, and the predictions of dedicated ACERMC-3.8 samples generated with different tuning parameters are compared to give the uncertainty related to the modelling of initial- and final-state radiation (ISR/FSR). At NLO, contributions with an additional bottom quark in the final state lead to ambiguities in the distinction between the Wt process ($gb \rightarrow Wtb$) and top-quark pair production. All the Wt samples, generated using MC@NLO-4.06 and POWHEG-BOX, use the diagram removal scheme [104] to model this interference. The

Table 9 Acceptance times efficiency for the various signal regions, for a few selected (scalar top, scalar tau) signal mass hypotheses. For each mass point, values are shown only for channels targeting that point. The lepton–lepton results are taken from Ref. [50]

$\tilde{t}_1$ mass [GeV]	$\tilde{\tau}_1$ mass [GeV]	Lepton–lepton $\mathcal{A} \times \epsilon$	Lepton–hadron $\mathcal{A} \times \epsilon$ (SRLM)	Lepton–hadron $\mathcal{A} \times \epsilon$ (SRHM)	Hadron–hadron $\mathcal{A} \times \epsilon$
153	87	–	1.29×10^{-4}	–	2.27×10^{-4}
195	87	–	1.36×10^{-4}	–	4.46×10^{-4}
195	148	1.71×10^{-4}	7.80×10^{-5}	–	7.00×10^{-4}
195	185	8.01×10^{-4}	–	–	–
391	148	7.32×10^{-4}	–	9.44×10^{-4}	3.40×10^{-3}
503	493	1.03×10^{-2}	–	–	–
561	87	–	–	1.74×10^{-3}	6.70×10^{-3}
561	337	–	–	1.30×10^{-2}	9.90×10^{-3}
561	500	–	–	8.68×10^{-3}	2.50×10^{-3}

ACERMC-3.8 event generator is used to simulate the WWb and $WWb\bar{b}$ final states at leading order (which include both the $t\bar{t}$ and Wt single-top-quark processes); the predictions of these ACERMC-3.8 samples are then compared to those of the nominal MC samples in order to assess the uncertainty on the background estimate from this interference. The uncertainties on W+jets and Z+jets production are evaluated by studying the predictions of ALPGEN-2.14 with various choices of the renormalisation and factorisation scales.

The impact of systematic uncertainties on the total background estimate in the different SRs is shown in Table 6. The table quotes, for each SR, the relative background uncertainty attributed to each source.

Signal cross sections are calculated at NLO+NLL with a total associated uncertainty between 14 and 16 % for scalar top masses between 150 and 560 GeV.

7 Results and interpretation

The numbers of events observed in the hadron–hadron SR and in the two lepton–hadron SRs are reported in Table 7, along with the background yields before and after the background-only likelihood fit. In both the results and interpretation tables (Tables 7, 8) the quoted uncertainties include all the sources of statistical and systematic uncertainty. Good agreement is seen between the observed yields and the background estimates.

Figure 7 shows the distributions of $m_{\mathrm{T}}^{\mathrm{sum}}(\tau_{\mathrm{had}}, \tau_{\mathrm{had}})$ and $m_{\mathrm{T2}}(\tau_{\mathrm{had}}, \tau_{\mathrm{had}})$ for the hadron–hadron channel, for events satisfying all the SR criteria except that on the variable being reported in the figure. Figure 8 shows $m_{\mathrm{T2}}(b\ell, b\tau_{\mathrm{had}})$ for the lepton–hadron low-mass selection and $m_{\mathrm{T2}}(\ell, \tau_{\mathrm{had}})$ for the lepton–hadron high-mass selection for events satisfying all the corresponding SR criteria except those on the variable displayed in the figure.

Upper limits at 95 % confidence level (CL) on the number of beyond-the-SM (BSM) events for each SR are derived

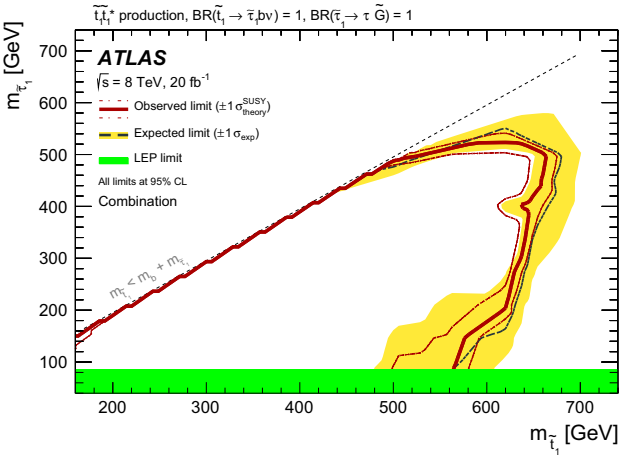

Fig. 9 Observed and expected exclusion contours at 95 % CL in the $(\tilde{t}_1, \tilde{\tau}_1)$ mass plane from the combination of all selections. The *dashed* and *solid lines* show the 95 % CL expected and observed limits, respectively, including all uncertainties except for the theoretical signal cross-section uncertainty (PDF and scale). The band around the expected limit shows the $\pm 1\sigma$ expectation. The *dotted* $\pm 1\sigma$ *lines* around the observed limit represent the results obtained when varying the nominal signal cross section up or down by the theoretical uncertainty. The LEP limit on the mass of the scalar tau is also shown

using the HistFitter program [105], with the CL_s likelihood ratio prescription as described in Ref. [106]. The limits are calculated for each SR separately, with the observed number of events, the expected background and the background uncertainty as input to the calculation. Possible signal contamination in the control regions is neglected. Dividing the limits on the number of BSM events by the integrated luminosity of the data sample, these can be interpreted as upper limits on the visible BSM cross section, $\sigma_{\mathrm{vis}} = \sigma \times \mathcal{A} \times \epsilon$, where σ is the production cross section for the BSM signal, $\mathcal{A}$ is the acceptance defined as the fraction of events passing the geometric and kinematic selections at particle level, and ϵ is the detector reconstruction, identification and trigger efficiency. Table 8 summarises, for each SR, the estimated SM background yields, the observed numbers of events, and the

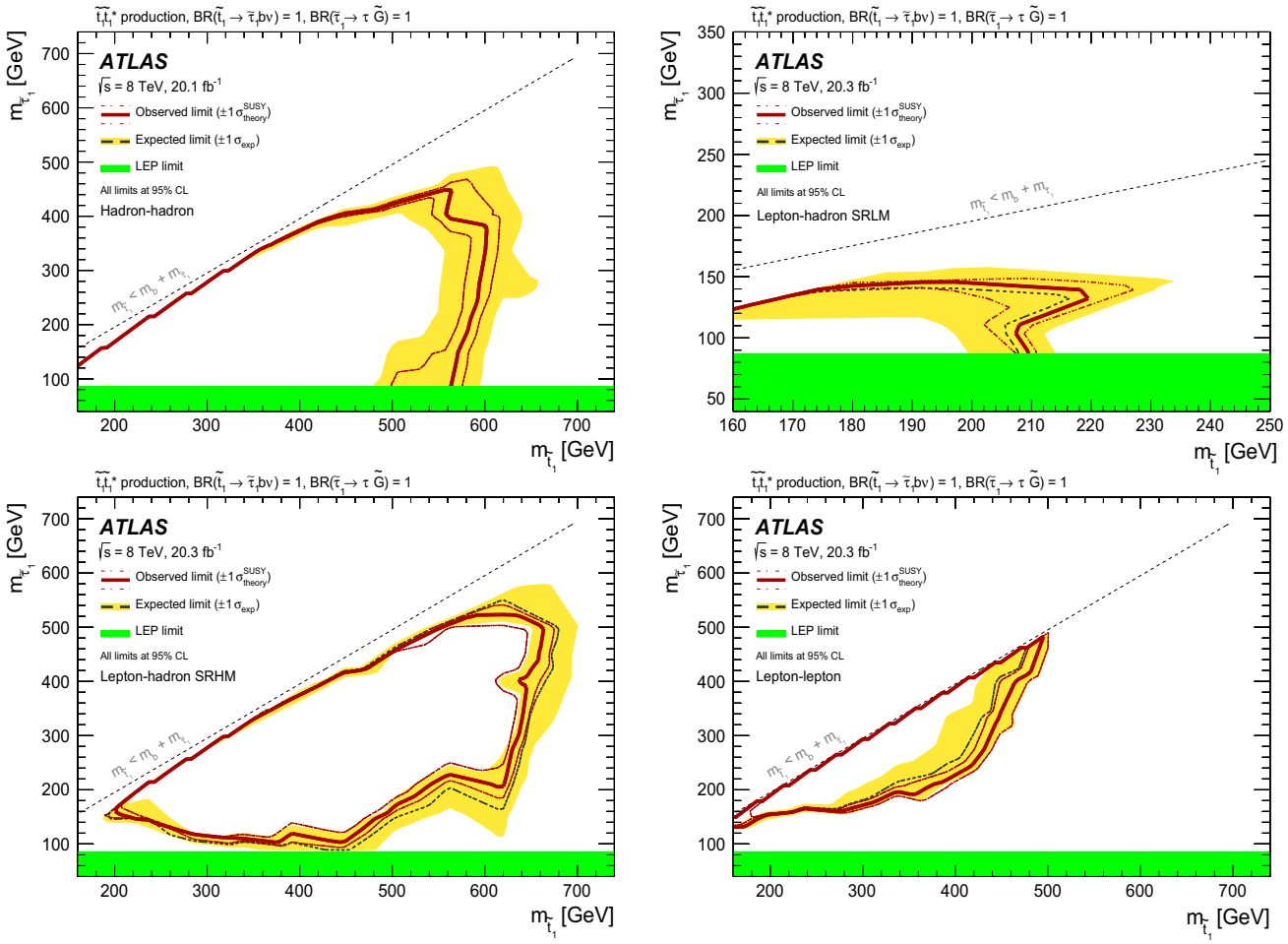

Fig. 10 Observed and expected exclusion contours at 95 % CL in the $(\tilde{t}_1, \tilde{\tau}_1)$ mass plane from the hadron–hadron (*top left*), the lepton–hadron low-mass (*top right*), the lepton–hadron high-mass (*bottom left*) and the lepton–lepton selections of Ref. [50] (*bottom right*). The *dashed* and *solid lines* show the 95 % CL expected and observed limits, respectively, including all uncertainties except for the theoretical signal cross-section uncertainty (PDF and scale). The band around the expected limit shows the $\pm 1\sigma$ expectation. The *dotted* $\pm 1\sigma$ *lines* around the observed limit represent the results obtained when varying the nominal signal cross section up or down by the theoretical uncertainty. The LEP limit on the mass of the scalar tau is also shown

expected and observed upper limits on event yields from a BSM signal and on σ_{vis}. Table 9 summarises, for each SR, the acceptance times efficiency for the relevant final state under various signal mass hypotheses.

Exclusion limits are derived for the scalar top pair production, assuming the $\tilde{t}_1$ decays with 100 % BR into $b\nu_\tau\tilde{\tau}_1$ and the $\tilde{\tau}_1$ decays into a tau lepton and a gravitino. The fit used for these limits is similar to that described in Sect. 5, but it now includes the expected signal in the likelihood, with an overall signal-strength parameter constrained to be positive. The CRs and SRs are fit simultaneously, taking into account the experimental and theoretical systematic uncertainties as nuisance parameters. The signal contamination in the CRs is also taken into account. Exclusion contours are set in the plane defined by the $\tilde{t}_1$ and $\tilde{\tau}_1$ masses.

Systematic uncertainties on the signal expectations stemming from detector effects are included in the fit in the same way as for the backgrounds. Systematic uncertainties on the signal cross section due to the choice of renormalisation and factorisation scales and PDF uncertainties are calculated as described in Sect. 6. Unlike other nuisance parameters, the signal cross-section uncertainties are only used to assess the impact of a $\pm 1\sigma$ variation on the observed limit.

For each mass hypothesis, the expected limits are calculated for the hadron–hadron selection, the two lepton–hadron selections, and the statistical combination of the lepton–lepton selections described in Ref. [50]. The selection giving the best expected sensitivity is used to compute the expected and observed CL_s value. The resulting exclusion contours are shown in Fig. 9. The limits for each individual channel are reported in Fig. 10. The black dashed and red solid lines show the 95 % CL expected and observed limits, respectively, including all uncertainties except for the theoretical signal cross-section uncertainty (PDF and scale). The yellow bands

around the expected limits show the $\pm 1\sigma$ expectations. The red dotted $\pm 1\sigma$ lines around the observed limit represent the results obtained when varying the nominal signal cross section up or down by its theoretical uncertainty. Numerical limits quoted on the particle masses are taken from these -1σ *theoretical lines*.

As can be seen from Fig. 9, models with a scalar top mass below 490 GeV are excluded. Depending on the scalar tau mass, some models with scalar top masses up to 650 GeV are also excluded. The scalar top masses below 150 GeV are not fully considered but they are unlikely to be viable because the cross section times branching ratio for $\tilde{t}_1\tilde{t}_1 \to b\tau b\tau + X$ is more than 25 times larger than the cross section times branching ratio for the production of $t\bar{t}$ decaying into the same di-tau final state, and measurements of the $t\bar{t}$ cross section in various final states [107–110] are in good agreement with the SM prediction.

8 Conclusion

A search for direct pair production of supersymmetric partners of the top quark decaying via a scalar tau to a nearly massless gravitino has been performed using 20 fb^{-1} of pp collision data at $\sqrt{s} = 8$ TeV, collected by the ATLAS experiment at the LHC in 2012. Scalar top candidates are searched for in events with either two hadronically decaying taus, one hadronically decaying tau and one light lepton, or two light leptons. Good agreement is observed between the Standard Model background estimate and the data. The first results from a hadron collider search for the three-body decay mode to the scalar tau are presented. In the context of the model considered, lower limits on the scalar top mass are set at 95 % confidence level, and found to be between 490 and 650 GeV for scalar tau masses ranging from the LEP limit to the scalar top mass.

Acknowledgments We thank CERN for the very successful operation of the LHC, as well as the support staff from our institutions without whom ATLAS could not be operated efficiently. We acknowledge the support of ANPCyT, Argentina; YerPhI, Armenia; ARC, Australia; BMWFW and FWF, Austria; ANAS, Azerbaijan; SSTC, Belarus; CNPq and FAPESP, Brazil; NSERC, NRC and CFI, Canada; CERN; CONICYT, Chile; CAS, MOST and NSFC, China; COLCIENCIAS, Colombia; MSMT CR, MPO CR and VSC CR, Czech Republic; DNRF, DNSRC and Lundbeck Foundation, Denmark; IN2P3-CNRS, CEA-DSM/IRFU, France; GNSF, Georgia; BMBF, HGF, and MPG, Germany; GSRT, Greece; RGC, Hong Kong SAR, China; ISF, I-CORE and Benoziyo Center, Israel; INFN, Italy; MEXT and JSPS, Japan; CNRST, Morocco; FOM and NWO, Netherlands; RCN, Norway; MNiSW and NCN, Poland; FCT, Portugal; MNE/IFA, Romania; MES of Russia and NRC KI, Russian Federation; JINR; MESTD, Serbia; MSSR, Slovakia; ARRS and MIZŠ, Slovenia; DST/NRF, South Africa; MINECO, Spain; SRC and Wallenberg Foundation, Sweden; SERI, SNSF and Cantons of Bern and Geneva, Switzerland; MOST, Taiwan; TAEK, Turkey; STFC, United Kingdom; DOE and NSF, United States of America. In addition, individual groups and members have received support from BCKDF, the Canada Council, CANARIE, CRC, Compute Canada, FQRNT, and the Ontario Innovation Trust, Canada; EPLANET, ERC, FP7, Horizon 2020 and Marie Skłodowska-Curie Actions, European Union; Investissements d'Avenir Labex and Idex, ANR, Region Auvergne and Fondation Partager le Savoir, France; DFG and AvH Foundation, Germany; Herakleitos, Thales and Aristeia programmes co-financed by EU-ESF and the Greek NSRF; BSF, GIF and Minerva, Israel; BRF, Norway; the Royal Society and Leverhulme Trust, United Kingdom. The crucial computing support from all WLCG partners is acknowledged gratefully, in particular from CERN and the ATLAS Tier-1 facilities at TRIUMF (Canada), NDGF (Denmark, Norway, Sweden), CC-IN2P3 (France), KIT/GridKA (Germany), INFN-CNAF (Italy), NL-T1 (Netherlands), PIC (Spain), ASGC (Taiwan), RAL (UK) and BNL (USA) and in the Tier-2 facilities worldwide.

References

1. S. Weinberg, Implications of dynamical symmetry breaking. Phys. Rev. D **13**, 974–996 (1976)
2. E. Gildener, Gauge symmetry hierarchies. Phys. Rev. D **14**, 1667 (1976)
3. S. Weinberg, Implications of dynamical symmetry breaking: an addendum. Phys. Rev. D **19**, 1277–1280 (1979)
4. L. Susskind, Dynamics of spontaneous symmetry breaking in the Weinberg–Salam theory. Phys. Rev. D **20**, 2619–2625 (1979)
5. H. Miyazawa, Baryon number changing currents. Prog. Theor. Phys. **36**(6), 1266–1276 (1966)
6. P. Ramond, Dual theory for free fermions. Phys. Rev. D **3**, 2415–2418 (1971)
7. Y. Golfand, E. Likhtman, Extension of the algebra of Poincare group generators and violation of p invariance. JETP Lett. **13**, 323–326 (1971)
8. A. Neveu, J.H. Schwarz, Factorizable dual model of pions. Nucl. Phys. B **31**, 86–112 (1971)
9. A. Neveu, J.H. Schwarz, Quark model of dual pions. Phys. Rev. D **4**, 1109–1111 (1971)
10. J. Gervais, B. Sakita, Field theory interpretation of supergauges in dual models. Nucl. Phys. B **34**, 632–639 (1971)
11. D. Volkov, V. Akulov, Is the neutrino a goldstone particle? Phys. Lett. B **46**, 109–110 (1973)
12. J. Wess, B. Zumino, A Lagrangian model invariant under supergauge transformations. Phys. Lett. B **49**, 52 (1974)
13. J. Wess, B. Zumino, Supergauge transformations in four-dimensions. Nucl. Phys. B **70**, 39–50 (1974)
14. L. Evans, P. Bryant, LHC machine. JINST **3**, S08001 (2008)
15. P. Fayet, Supersymmetry and weak, electromagnetic and strong interactions. Phys. Lett. B **64**, 159 (1976)
16. P. Fayet, Spontaneously broken supersymmetric theories of weak, electromagnetic and strong interactions. Phys. Lett. B **69**, 489 (1977)
17. G.R. Farrar, P. Fayet, Phenomenology of the production, decay, and detection of new hadronic states associated with supersymmetry. Phys. Lett. B **76**, 575–579 (1978)
18. P. Fayet, Relations between the masses of the superpartners of leptons and quarks, the goldstino couplings and the neutral currents. Phys. Lett. B **84**, 416 (1979)

19. S. Dimopoulos, H. Georgi, Softly broken supersymmetry and SU(5). Nucl. Phys. B **193**, 150 (1981)
20. M. Dine, W. Fischler, A phenomenological model of particle physics based on supersymmetry. Phys. Lett. B **110**, 227 (1982)
21. L. Alvarez-Gaume, M. Claudson, M.B. Wise, Low-energy supersymmetry. Nucl. Phys. B **207**, 96 (1982)
22. C.R. Nappi, B.A. Ovrut, Supersymmetric extension of the $SU(3) \times SU(2) \times U(1)$ model. Phys. Lett. B **113**, 175 (1982)
23. M. Dine, A.E. Nelson, Dynamical supersymmetry breaking at low-energies. Phys. Rev. D **48**, 1277–1287 (1993). arXiv:hep-ph/9303230
24. M. Dine, A.E. Nelson, Y. Shirman, Low-energy dynamical supersymmetry breaking simplified. Phys. Rev. D **51**, 1362–1370 (1995). arXiv:hep-ph/9408384
25. M. Dine et al., New tools for low-energy dynamical supersymmetry breaking. Phys. Rev. D **53**, 2658–2669 (1996). arXiv:hep-ph/9507378
26. R. Barbieri, G. Giudice, Upper bounds on supersymmetric particle masses. Nucl. Phys. B **306**, 63 (1988)
27. M. Asano et al., Natural Supersymmetry at the LHC. JHEP **1012**, 019 (2010). arXiv:1010.0692 [hep-ph]
28. ATLAS Collaboration, ATLAS Run 1 searches for direct pair production of third-generation squarks at the Large Hadron Collider. EPJC (2015) (submitted). arXiv:1506.0861 [hep-ex]
29. C.M.S. Collaboration, Inclusive search for supersymmetry using the razor variables in pp collisions at $\sqrt{s} = 7$ TeV. Phys. Rev. Lett. **111**, 081802 (2013). arXiv:1212.6961 [hep-ex]
30. CMS Collaboration, Search for supersymmetry in hadronic final states with missing transverse energy using the variables α_T and b-quark multiplicity in pp collisions at 8 TeV. Eur. Phys. J. C **73**, 2568 (2013). arXiv:1303.2985 [hep-ex]
31. CMS Collaboration, Search for top-squark pair production in the single-lepton final state in pp collisions at $\sqrt{s} = 8TeV$. Eur. Phys. J. C **73**, 2677 (2013). arXiv:1308.1586 [hep-ex]
32. CMS Collaboration, Search for supersymmetry using razor variables in events with b-tagged jets in pp collisions at $\sqrt{s} = 8$ TeV. Phys. Rev. D **91**, 052018 (2015). arXiv:1502.00300 [hep-ex]
33. CMS Collaboration, Searches for supersymmetry using the M_{T2} variable in hadronic events produced in pp collisions at 8 TeV. JHEP **1505**, 078 (2015). arXiv:1502.04358 [hep-ex]
34. CMS Collaboration, Searches for third-generation squark production in fully hadronic final states in proton–proton collisions at $\sqrt{s} = 8$ TeV. JHEP **1506**, 116 (2015). arXiv:1503.08037 [hep-ex]
35. A. Arbey et al., Implications of a 125 GeV Higgs for supersymmetric models. Phys. Lett. B **708**, 162–169 (2012). arXiv:1112.3028 [hep-ph]
36. ATLAS and CMS Collaborations, Combined measurement of the Higgs boson mass in pp collisions at $\sqrt{s} = 7$ and 8 TeV with the ATLAS and CMS experiments. Phys. Rev. Lett. **114**, 191803 (2015). arXiv:1503.07589 [hep-ex]
37. N. Craig, D. Green, A. Katz, (De)Constructing a natural and flavorful supersymmetric standard model. JHEP **1107**, 045 (2011). arXiv:1103.3708 [hep-ph]
38. V.M. Abazov et al. (D0 Collaboration), Search for the lightest scalar top quark in events with two leptons in $p\overline{p}$. Phys. Lett. B **675**, 289–296 (2009). arXiv:0811.0459 [hep-ex]
39. C. Csaki, L. Randall, J. Terning, Light stops from Seiberg duality. Phys. Rev. D **86**, 075009 (2012). arXiv:1201.1293 [hep-ph]
40. G. Larsen, Y. Nomura, H.L. Roberts, Supersymmetry with light stops. JHEP **1206**, 032 (2012). arXiv:1202.6339 [hep-ph]
41. N. Craig, S. Dimopoulos, T. Gherghetta, Split families unified. JHEP **1204**, 116 (2012). arXiv:1203.0572 [hep-ph]
42. The LEP SUSY Working Group and ALEPH, DELPHI, L3, OPAL experiments, Combined LEP selectron/smuon/stau results, 183–208 GeV (2004). http://lepsusy.web.cern.ch/lepsusy/www/sleptons_summer04/slep_final.html
43. G. Abbiendi et al. (OPAL Collaboration), Searches for gauge-mediated supersymmetry breaking topologies in $e+e-$ collisions at LEP2. Eur. Phys. J. C **46**, 307–341 (2006). arXiv:hep-ex/0507048 [hep-ex]
44. A. Heister et al. (ALEPH Collaboration), Search for scalar leptons in $e+e-$ collisions at center-of-mass energies up to 209 GeV. Phys. Lett. B **526**, 206–220 (2002). arXiv:hep-ex/0112011 [hep-ex]
45. J. Abdallah et al. (DELPHI Collaboration), Searches for supersymmetric particles in $e+e-$ collisions up to 208 GeV and interpretation of the results within the MSSM. Eur. Phys. J. C **31**, 421–479 (2003). arXiv:hep-ex/0311019 [hep-ex]
46. P. Achard et al. (L3 Collaboration), Search for scalar leptons and scalar quarks at LEP. Phys. Lett. B **580**, 37–49 (2004). arXiv:hep-ex/0310007 [hep-ex]
47. ATLAS Collaboration, Search for direct top squark pair production in events with a Z boson, b-jets and missing transverse momentum in $\sqrt{s} = 8$ TeV pp collisions with the ATLAS detector. Eur. Phys. J. C **74**, 2883 (2014). arXiv:1403.5222 [hep-ex]
48. CMS Collaboration, Search for top squark and higgsino production using diphoton Higgs boson decays. Phys. Rev. Lett. **112**, 161802 (2014). arXiv:1312.3310 [hep-ex]
49. CMS Collaboration, Search for top-squark pairs decaying into Higgs or Z bosons in pp collisions at $\sqrt{s} = 8$ TeV. Phys. Lett. B **736**, 371 (2014). arXiv:1405.3886 [hep-ex]
50. ATLAS Collaboration, Search for direct top-squark pair production in final states with two leptons in pp collisions at $\sqrt{s} = 8$ TeV with the ATLAS detector. JHEP **1406**, 124 (2014). arXiv:1403.4853 [hep-ex]
51. ATLAS Collaboration, The ATLAS experiment at the CERN large hadron collider. JINST **3**, S08003 (2008)
52. ATLAS Collaboration, The ATLAS simulation infrastructure. Eur. Phys. J. C **70**, 823–874 (2010). arXiv:1005.4568 [physics.ins-det]
53. S. Agostinelli et al. (GEANT4 Collaboration), GEANT4: a simulation toolkit. Nucl. Instrum. Methods A **506**, 250–303 (2003)
54. ATLAS Collaboration, The simulation principle and performance of the ATLAS fast calorimeter simulation FastCaloSim, ATL-PHYS-PUB-2010-013 (2010). https://cdsweb.cern.ch/record/1300517
55. M. Bähr et al., Herwig++ physics and manual. Eur. Phys. J. C **58**, 639–707 (2008). 143 pages, program and additional information available from http://projects.hepforge.org/herwig. arXiv:0803.0883 [hep-ph]
56. P.M. Nadolsky et al., Implications of CTEQ global analysis for collider observables. Phys. Rev. D **78**, 013004 (2008). arXiv:0802.0007 [hep-ph]
57. W. Beenakker et al., Stop production at hadron colliders. Nucl. Phys. B **515**, 3–14 (1998). arXiv:hep-ph/9710451 [hep-ph]
58. W. Beenakker et al., Supersymmetric top and bottom squark production at hadron colliders. JHEP **1008**, 098 (2010). arXiv:1006.4771 [hep-ph]
59. W. Beenakker et al., Squark and gluino hadroproduction. Int. J. Mod. Phys. A **26**, 2637–2664 (2011). arXiv:1105.1110 [hep-ph]
60. M. Krämer et al., Supersymmetry production cross sections in pp collisions at $\sqrt{s} = 7$ TeV (2012). arXiv:1206.2892 [hep-ph]
61. S. Alioli et al., A general framework for implementing NLO calculations in shower Monte Carlo programs: the POWHEG BOX. JHEP **1006**, 043 (2010). arXiv:1002.2581 [hep-ph]
62. J.M. Campbell et al., Top-pair production and decay at NLO matched with parton showers. JHEP **1504**, 114 (2015). arXiv:1412.1828 [hep-ph]

63. T. Sjöstrand, S. Mrenna, P.Z. Skands, A brief introduction to PYTHIA 8.1. Comput. Phys. Common. **178**, 852–867 (2008). arXiv:0710.3820 [hep-ph]
64. M. Cacciari et al., Top-pair production at hadron colliders with next-to-next-to-leading logarithmic soft-gluon resummation. Phys. Lett. B **710**, 612–622 (2012). arXiv:1111.5869 [hep-ph]
65. P. Bärnreuther, M. Czakon, A. Mitov, Percent level precision physics at the Tevatron: first genuine NNLO QCD corrections to $q\bar{q} \rightarrow t\bar{t} + X$. Phys. Rev. Lett. **109**, 132001 (2012). arXiv:1204.5201 [hep-ph]
66. M. Czakon, A. Mitov, NNLO corrections to top-pair production at hadron colliders: the all-fermionic scattering channels. JHEP **1212**, 054 (2012). arXiv:1207.0236 [hep-ph]
67. M. Czakon, A. Mitov, NNLO corrections to top pair production at hadron colliders: the quark-gluon reaction. JHEP **1301**, 080 (2013). arXiv:1210.6832 [hep-ph]
68. M. Czakon, P. Fiedler, A. Mitov, The total top quark pair production cross-section at hadron colliders through $O(\alpha_S^4)$. Phys. Rev. Lett. **110**, 252004 (2013). arXiv:1303.6254 [hep-ph]
69. M. Czakon, A. Mitov, Top++: a program for the calculation of the top-pair cross-section at hadron colliders (2011). arXiv:1112.5675 [hep-ph]
70. J. Gao et al., The CT10 NNLO global analysis of QCD (2013). arXiv:1302.6246 [hep-ph]
71. B. Cooper et al., Importance of a consistent choice of alpha(s) in the matching of AlpGen and Pythia. Eur. Phys. J. C **72**, 2078 (2012). arXiv:1109.5295 [hep-ph]
72. E. Re, Single-top Wt-channel production matched with parton showers using the POWHEG method. Eur. Phys. J. C **71**, 1547 (2011). arXiv:1009.2450 [hep-ph]
73. S. Alioli et al., NLO single-top production matched with shower in POWHEG: s- and t-channel contributions. JHEP **0909**, 111 (2009). arXiv:0907.4076 [hep-ph]
74. N. Kidonakis, Two-loop soft anomalous dimensions for single top quark associated production with a $W-$ or $H-$. Phys. Rev. D **82**, 054018 (2010). arXiv:1005.4451 [hep-ph]
75. B.P. Kersevan, E. Richter-Was, The Monte Carlo event generator AcerMC version 2.0 with interfaces to PYTHIA 6.2 and HERWIG 6.5 (2004). arXiv:hep-ph/0405247 [hep-ph]
76. N. Kidonakis, Next-to-next-to-leading-order collinear and soft gluon corrections for t-channel single top quark production. Phys. Rev. D **83**, 091503 (2011). arXiv:1103.2792 [hep-ph]
77. J. Alwall et al., MadGraph 5: going beyond. JHEP **06**, 128 (2011). arXiv:1106.522 [hep-ph]
78. M. Garzelli et al., $t\bar{t}W^{+-}$ and $t\bar{t}Z$ hadroproduction at NLO accuracy in QCD with parton shower and hadronization effects. JHEP **11**, 056 (2012). arXiv:1208.2665 [hep-ph]
79. ATLAS Collaboration, New ATLAS event generator tunes to 2010 data (). http://cdsweb.cern.ch/record/1345343
80. T. Gleisberg et al., Event generation with SHERPA 1.1. JHEP **0902**, 007 (2009). arXiv:0811.4622 [hep-ph]
81. T. Binoth et al., Gluon-induced W-boson pair production at the LHC. JHEP **0612**, 046 (2006). arXiv:hep-ph/0611170 [hep-ph]
82. M.L. Mangano et al., ALPGEN, a generator for hard multiparton processes in hadronic collisions. JHEP **0307**, 001 (2003). arXiv:hep-ph/0206293 [hep-ph]
83. G. Corcella et al., HERWIG 6: an event generator for hadron emission reactions with interfering gluons (including supersymmetric processes). JHEP **0101**, 010 (2001). arXiv:hep-ph/0011363 [hep-ph]
84. S. Catani et al., Vector boson production at hadron colliders: a fully exclusive QCD calculation at NNLO. Phys. Rev. Lett. **103**, 082001 (2009). arXiv:0903.2120 [hep-ph]
85. S. Gieseke, C. Rohr, A. Siodmok, Colour reconnections in Herwig++. Eur. Phys. J. C **72**, 2225 (2012). arXiv:1206.0041 [hep-ph]
86. ATLAS Collaboration, Performance of the ATLAS trigger system in 2010. Eur. Phys. J. C **72**, 1849 (2012). arXiv:1110.1530 [hep-ex]
87. ATLAS Collaboration, Improved luminosity determination in pp collisions at $\sqrt{s} = 7$ TeV using the ATLAS detector at the LHC. Eur. Phys. J. C **73**, 2518 (2013). arXiv:1302.4393 [hep-ex]
88. M. Cacciari, G.P. Salam, G. Soyez, The anti-k(t) jet clustering algorithm. JHEP **0804**, 063 (2008). arXiv:0802.1189 [hep-ph]
89. M. Cacciari, G.P. Salam, Dispelling the N^3 myth for the k_t jet-finder. Phys. Lett. B **641**, 57–61 (2006). arXiv:hep-ph/0512210 [hep-ph]
90. ATLAS Collaboration, Expected performance of the ATLAS experiment—detector, trigger and physics. CERN-OPEN-2008-020 (2009). arXiv:0901.0512 [hep-ex]
91. M. Cacciari, G.P. Salam, G. Soyez, The catchment area of jets. JHEP **0804**, 005 (2008). arXiv:0802.1188 [hep-ph]
92. ATLAS Collaboration, Jet energy measurement with the ATLAS detector in proton–proton collisions at $\sqrt{s} = 7$ TeV. Eur. Phys. J. C **73**, 2304 (2013). arXiv:1112.6426 [hep-ex]
93. ATLAS Collaboration, Single hadron response measurement and calorimeter jet energy scale uncertainty with the ATLAS detector at the LHC. Eur. Phys. J. C **73**, 2305 (2013). arXiv:1203.1302 [hep-ex]
94. ATLAS Collaboration, Characterisation and mitigation of beam-induced backgrounds observed in the ATLAS detector during the 2011 proton–proton run. JINST **8**, P07004 (2013). arXiv:1303.0223 [hep-ex]
95. ATLAS Collaboration, Calibration of b-tagging using dileptonic top pair events in a combinatorial likelihood approach with the ATLAS experiment. ATLAS-CONF-2014-004 (2014). https://cdsweb.cern.ch/record/1664335
96. ATLAS Collaboration, Calibration of the performance of b-tagging for c and light-flavour jets in the 2012 ATLAS data. ATLAS-CONF-2014-046 (2014). http://cdsweb.cern.ch/record/1741020
97. ATLAS Collaboration, Electron reconstruction and identification efficiency measurements with the ATLAS detector using the 2011 LHC proton–proton collision data. Eur. Phys. J. C **74**, 2941 (2014). arXiv:1404.2240 [hep-ex]
98. ATLAS Collaboration, Measurement of the muon reconstruction performance of the ATLAS detector using 2011 and 2012 LHC proton–proton collision data. Eur. Phys. J. C **74**, 3130 (2014). arXiv:1407.3935 [hep-ex]
99. ATLAS Collaboration, Identification and energy calibration of hadronically decaying tau leptons with the ATLAS experiment in pp collisions at $\sqrt{s} = 8$ TeV. Eur. Phys. J. C **75**, 303 (2015). arXiv:1412.7086 [hep-ex]
100. ATLAS Collaboration, Performance of missing transverse momentum reconstruction in proton–proton collisions at 7 TeV with ATLAS. Eur. Phys. J. C **72**, 1844 (2012). arXiv:1108.5602 [hep-ex]
101. C.G. Lester, D.J. Summers, Measuring masses of semi-invisibly decaying particles pair produced at hadron colliders. Phys. Lett. B **463**, 99–103 (1999). arXiv:hep-ph/9906349
102. A. Barr, C. Lester, P. Stephens, m(T2): The truth behind the glamour. J. Phys. G **29**, 2343–2363 (2003). arXiv:hep-ph/0304226
103. ATLAS Collaboration, Search for squarks and gluinos with the ATLAS detector in final states with jets and missing transverse momentum using 4.7 fb^1 proton–proton collision data. Phys. Rev. D **87**, 012008 (2013). arXiv:1208.0949 [hep-ex]
104. S. Frixione et al., Single-top hadroproduction in association with a W boson. JHEP **0807**, 029 (2008). arXiv:0805.3067 [hep-ph]
105. M. Baak et al., HistFitter software framework for statistical data analysis. Eur. Phys. J. C **75**, 153 (2015). arXiv:1410.1280 [hep-ph]

106. A.L. Read, Presentation of search results: the CL(s) technique. J. Phys. G **28**, 2693–2704 (2002)
107. ATLAS Collaboration, Measurement of the top quark pair cross section with ATLAS in pp collisions at $\sqrt{s} = 7TeV$ using final states with an electron or a muon and a hadronically decaying τ lepton. Phys. Lett. B **717**, 89 (2012). arXiv:1205.2067 [hep-ex]
108. CMS Collaboration, Measurement of the $t\bar{t}$ production cross section in pp collisions at $\sqrt{s} = 8$ TeV in dilepton final states containing one τ lepton. Phys. Lett. B **739**, 23–43 (2014)
109. ATLAS Collaboration, Measurement of the $t\bar{t}$ production cross section in the tau+jets channel using the ATLAS detector. Eur. Phys. J. C **73**, 2328 (2013). arXiv:1211.7205 [hep-ex]
110. CMS Collaboration, Measurement of the top-antitop production cross section in the tau+jets channel in pp collisions at $\sqrt{s} = 7$ TeV. Eur. Phys. J. C **73**, 2386 (2013). arXiv:1301.5755 [hep-ex]

ATLAS Collaboration

G. Aad[85], B. Abbott[113], J. Abdallah[151], O. Abdinov[11], R. Aben[107], M. Abolins[90], O. S. AbouZeid[158], H. Abramowicz[153], H. Abreu[152], R. Abreu[116], Y. Abulaiti[146a,146b], B. S. Acharya[164a,164b,a], L. Adamczyk[38a], D. L. Adams[25], J. Adelman[108], S. Adomeit[100], T. Adye[131], A. A. Affolder[74], T. Agatonovic-Jovin[13], J. Agricola[54], J. A. Aguilar-Saavedra[126a,126f], S. P. Ahlen[22], F. Ahmadov[65,b], G. Aielli[133a,133b], H. Akerstedt[146a,146b], T. P. A. Åkesson[81], A. V. Akimov[96], G. L. Alberghi[20a,20b], J. Albert[169], S. Albrand[55], M. J. Alconada Verzini[71], M. Aleksa[30], I. N. Aleksandrov[65], C. Alexa[26a], G. Alexander[153], T. Alexopoulos[10], M. Alhroob[113], G. Alimonti[91a], L. Alio[85], J. Alison[31], S. P. Alkire[35], B. M. M. Allbrooke[149], P. P. Allport[74], A. Aloisio[104a,104b], A. Alonso[36], F. Alonso[71], C. Alpigiani[76], A. Altheimer[35], B. Alvarez Gonzalez[30], D. Álvarez Piqueras[167], M. G. Alviggi[104a,104b], B. T. Amadio[15], K. Amako[66], Y. Amaral Coutinho[24a], C. Amelung[23], D. Amidei[89], S. P. Amor Dos Santos[126a,126c], A. Amorim[126a,126b], S. Amoroso[48], N. Amram[153], G. Amundsen[23], C. Anastopoulos[139], L. S. Ancu[49], N. Andari[108], T. Andeen[35], C. F. Anders[58b], G. Anders[30], J. K. Anders[74], K. J. Anderson[31], A. Andreazza[91a,91b], V. Andrei[58a], S. Angelidakis[9], I. Angelozzi[107], P. Anger[44], A. Angerami[35], F. Anghinolfi[30], A. V. Anisenkov[109,c], N. Anjos[12], A. Annovi[124a,124b], M. Antonelli[47], A. Antonov[98], J. Antos[144b], F. Anulli[132a], M. Aoki[66], L. Aperio Bella[18], G. Arabidze[90], Y. Arai[66], J. P. Araque[126a], A. T. H. Arce[45], F. A. Arduh[71], J-F. Arguin[95], S. Argyropoulos[42], M. Arik[19a], A. J. Armbruster[30], O. Arnaez[30], V. Arnal[82], H. Arnold[48], M. Arratia[28], O. Arslan[21], A. Artamonov[97], G. Artoni[23], S. Asai[155], N. Asbah[42], A. Ashkenazi[153], B. Åsman[146a,146b], L. Asquith[149], K. Assamagan[25], R. Astalos[144a], M. Atkinson[165], N. B. Atlay[141], K. Augsten[128], M. Aurousseau[145b], G. Avolio[30], B. Axen[15], M. K. Ayoub[117], G. Azuelos[95,d], M. A. Baak[30], A. E. Baas[58a], M. J. Baca[18], C. Bacci[134a,134b], H. Bachacou[136], K. Bachas[154], M. Backes[30], M. Backhaus[30], P. Bagiacchi[132a,132b], P. Bagnaia[132a,132b], Y. Bai[33a], T. Bain[35], J. T. Baines[131], O. K. Baker[176], E. M. Baldin[109,c], P. Balek[129], T. Balestri[148], F. Balli[84], E. Banas[39], Sw. Banerjee[173], A. A. E. Bannoura[175], H. S. Bansil[18], L. Barak[30], E. L. Barberio[88], D. Barberis[50a,50b], M. Barbero[85], T. Barillari[101], M. Barisonzi[164a,164b], T. Barklow[143], N. Barlow[28], S. L. Barnes[84], B. M. Barnett[131], R. M. Barnett[15], Z. Barnovska[5], A. Baroncelli[134a], G. Barone[23], A. J. Barr[120], F. Barreiro[82], J. Barreiro Guimarães da Costa[57], R. Bartoldus[143], A. E. Barton[72], P. Bartos[144a], A. Basalaev[123], A. Bassalat[117], A. Basye[165], R. L. Bates[53], S. J. Batista[158], J. R. Batley[28], M. Battaglia[137], M. Bauce[132a,132b], F. Bauer[136], H. S. Bawa[143,e], J. B. Beacham[111], M. D. Beattie[72], T. Beau[80], P. H. Beauchemin[161], R. Beccherle[124a,124b], P. Bechtle[21], H. P. Beck[17,f], K. Becker[120], M. Becker[83], S. Becker[100], M. Beckingham[170], C. Becot[117], A. J. Beddall[19b], A. Beddall[19b], V. A. Bednyakov[65], C. P. Bee[148], L. J. Beemster[107], T. A. Beermann[175], M. Begel[25], J. K. Behr[120], C. Belanger-Champagne[87], W. H. Bell[49], G. Bella[153], L. Bellagamba[20a], A. Bellerive[29], M. Bellomo[86], K. Belotskiy[98], O. Beltramello[30], O. Benary[153], D. Benchekroun[135a], M. Bender[100], K. Bendtz[146a,146b], N. Benekos[10], Y. Benhammou[153], E. Benhar Noccioli[49], J. A. Benitez Garcia[159b], D. P. Benjamin[45], J. R. Bensinger[23], S. Bentvelsen[107], L. Beresford[120], M. Beretta[47], D. Berge[107], E. Bergeaas Kuutmann[166], N. Berger[5], F. Berghaus[169], J. Beringer[15], C. Bernard[22], N. R. Bernard[86], C. Bernius[110], F. U. Bernlochner[21], T. Berry[77], P. Berta[129], C. Bertella[83], G. Bertoli[146a,146b], F. Bertolucci[124a,124b], C. Bertsche[113], D. Bertsche[113], M. I. Besana[91a], G. J. Besjes[36], O. Bessidskaia Bylund[146a,146b], M. Bessner[42], N. Besson[136], C. Betancourt[48], S. Bethke[101], A. J. Bevan[76], W. Bhimji[15], R. M. Bianchi[125], L. Bianchini[23], M. Bianco[30], O. Biebel[100], D. Biedermann[16], S. P. Bieniek[78], M. Biglietti[134a], J. Bilbao De Mendizabal[49], H. Bilokon[47], M. Bindi[54], S. Binet[117], A. Bingul[19b], C. Bini[132a,132b], S. Biondi[20a,20b], C. W. Black[150], J. E. Black[143], K. M. Black[22], D. Blackburn[138], R. E. Blair[6], J.-B. Blanchard[136], J. E. Blanco[77], T. Blazek[144a], I. Bloch[42], C. Blocker[23], W. Blum[83,*], U. Blumenschein[54], G. J. Bobbink[107], V. S. Bobrovnikov[109,c], S. S. Bocchetta[81], A. Bocci[45], C. Bock[100], M. Boehler[48], J. A. Bogaerts[30], D. Bogavac[13], A. G. Bogdanchikov[109], C. Bohm[146a], V. Boisvert[77], T. Bold[38a], V. Boldea[26a], A. S. Boldyrev[99], M. Bomben[80], M. Bona[76], M. Boonekamp[136], A. Borisov[130], G. Borissov[72], S. Borroni[42], J. Bortfeldt[100], V. Bortolotto[60a,60b,60c], K. Bos[107], D. Boscherini[20a], M. Bosman[12], J. Boudreau[125], J. Bouffard[2], E. V. Bouhova-Thacker[72], D. Boumediene[34], C. Bourdarios[117], N. Bousson[114],

A. Boveia[30], J. Boyd[30], I. R. Boyko[65], I. Bozic[13], J. Bracinik[18], A. Brandt[8], G. Brandt[54], O. Brandt[58a], U. Bratzler[156], B. Brau[86], J. E. Brau[116], H. M. Braun[175,*], S. F. Brazzale[164a,164c], W. D. Breaden Madden[53], K. Brendlinger[122], A. J. Brennan[88], L. Brenner[107], R. Brenner[166], S. Bressler[172], K. Bristow[145c], T. M. Bristow[46], D. Britton[53], D. Britzger[42], F. M. Brochu[28], I. Brock[21], R. Brock[90], J. Bronner[101], G. Brooijmans[35], T. Brooks[77], W. K. Brooks[32b], J. Brosamer[15], E. Brost[116], J. Brown[55], P. A. Bruckman de Renstrom[39], D. Bruncko[144b], R. Bruneliere[48], A. Bruni[20a], G. Bruni[20a], M. Bruschi[20a], N. Bruscino[21], L. Bryngemark[81], T. Buanes[14], Q. Buat[142], P. Buchholz[141], A. G. Buckley[53], S. I. Buda[26a], I. A. Budagov[65], F. Buehrer[48], L. Bugge[119], M. K. Bugge[119], O. Bulekov[98], D. Bullock[8], H. Burckhart[30], S. Burdin[74], C. D. Burgard[48], B. Burghgrave[108], S. Burke[131], I. Burmeister[43], E. Busato[34], D. Büscher[48], V. Büscher[83], P. Bussey[53], J. M. Butler[22], A. I. Butt[3], C. M. Buttar[53], J. M. Butterworth[78], P. Butti[107], W. Buttinger[25], A. Buzatu[53], A. R. Buzykaev[109,c], S. Cabrera Urbán[167], D. Caforio[128], V. M. Cairo[37a,37b], O. Cakir[4a], N. Calace[49], P. Calafiura[15], A. Calandri[136], G. Calderini[80], P. Calfayan[100], L. P. Caloba[24a], D. Calvet[34], S. Calvet[34], R. Camacho Toro[31], S. Camarda[42], P. Camarri[133a,133b], D. Cameron[119], R. Caminal Armadans[165], S. Campana[30], M. Campanelli[78], A. Campoverde[148], V. Canale[104a,104b], A. Canepa[159a], M. Cano Bret[33e], J. Cantero[82], R. Cantrill[126a], T. Cao[40], M. D. M. Capeans Garrido[30], I. Caprini[26a], M. Caprini[26a], M. Capua[37a,37b], R. Caputo[83], R. Cardarelli[133a], F. Cardillo[48], T. Carli[30], G. Carlino[104a], L. Carminati[91a,91b], S. Caron[106], E. Carquin[32a], G. D. Carrillo-Montoya[30], J. R. Carter[28], J. Carvalho[126a,126c], D. Casadei[78], M. P. Casado[12], M. Casolino[12], E. Castaneda-Miranda[145b], A. Castelli[107], V. Castillo Gimenez[167], N. F. Castro[126a,g], P. Catastini[57], A. Catinaccio[30], J. R. Catmore[119], A. Cattai[30], J. Caudron[83], V. Cavaliere[165], D. Cavalli[91a], M. Cavalli-Sforza[12], V. Cavasinni[124a,124b], F. Ceradini[134a,134b], B. C. Cerio[45], K. Cerny[129], A. S. Cerqueira[24b], A. Cerri[149], L. Cerrito[76], F. Cerutti[15], M. Cerv[30], A. Cervelli[17], S. A. Cetin[19c], A. Chafaq[135a], D. Chakraborty[108], I. Chalupkova[129], P. Chang[165], J. D. Chapman[28], D. G. Charlton[18], C. C. Chau[158], C. A. Chavez Barajas[149], S. Cheatham[152], A. Chegwidden[90], S. Chekanov[6], S. V. Chekulaev[159a], G. A. Chelkov[65,h], M. A. Chelstowska[89], C. Chen[64], H. Chen[25], K. Chen[148], L. Chen[33d,i], S. Chen[33c], X. Chen[33f], Y. Chen[67], H. C. Cheng[89], Y. Cheng[31], A. Cheplakov[65], E. Cheremushkina[130], R. Cherkaoui El Moursli[135e], V. Chernyatin[25,*], E. Cheu[7], L. Chevalier[136], V. Chiarella[47], G. Chiarelli[124a,124b], G. Chiodini[73a], A. S. Chisholm[18], R. T. Chislett[78], A. Chitan[26a], M. V. Chizhov[65], K. Choi[61], S. Chouridou[9], B. K. B. Chow[100], V. Christodoulou[78], D. Chromek-Burckhart[30], J. Chudoba[127], A. J. Chuinard[87], J. J. Chwastowski[39], L. Chytka[115], G. Ciapetti[132a,132b], A. K. Ciftci[4a], D. Cinca[53], V. Cindro[75], I. A. Cioara[21], A. Ciocio[15], F. Cirotto[104a,104b], Z. H. Citron[172], M. Ciubancan[26a], A. Clark[49], B. L. Clark[57], P. J. Clark[46], R. N. Clarke[15], W. Cleland[125], C. Clement[146a,146b], Y. Coadou[85], M. Cobal[164a,164c], A. Coccaro[49], J. Cochran[64], L. Coffey[23], J. G. Cogan[143], L. Colasurdo[106], B. Cole[35], S. Cole[108], A. P. Colijn[107], J. Collot[55], T. Colombo[58c], G. Compostella[101], P. Conde Muiño[126a,126b], E. Coniavitis[48], S. H. Connell[145b], I. A. Connelly[77], V. Consorti[48], S. Constantinescu[26a], C. Conta[121a,121b], G. Conti[30], F. Conventi[104a,j], M. Cooke[15], B. D. Cooper[78], A. M. Cooper-Sarkar[120], T. Cornelissen[175], M. Corradi[20a], F. Corriveau[87,k], A. Corso-Radu[163], A. Cortes-Gonzalez[12], G. Cortiana[101], G. Costa[91a], M. J. Costa[167], D. Costanzo[139], D. Côté[8], G. Cottin[28], G. Cowan[77], B. E. Cox[84], K. Cranmer[110], G. Cree[29], S. Crépé-Renaudin[55], F. Crescioli[80], W. A. Cribbs[146a,146b], M. Crispin Ortuzar[120], M. Cristinziani[21], V. Croft[106], G. Crosetti[37a,37b], T. Cuhadar Donszelmann[139], J. Cummings[176], M. Curatolo[47], C. Cuthbert[150], H. Czirr[141], P. Czodrowski[3], S. D'Auria[53], M. D'Onofrio[74], M. J. Da Cunha Sargedas De Sousa[126a,126b], C. Da Via[84], W. Dabrowski[38a], A. Dafinca[120], T. Dai[89], O. Dale[14], F. Dallaire[95], C. Dallapiccola[86], M. Dam[36], J. R. Dandoy[31], N. P. Dang[48], A. C. Daniells[18], M. Danninger[168], M. Dano Hoffmann[136], V. Dao[48], G. Darbo[50a], S. Darmora[8], J. Dassoulas[3], A. Dattagupta[61], W. Davey[21], C. David[169], T. Davidek[129], E. Davies[120,l], M. Davies[153], P. Davison[78], Y. Davygora[58a], E. Dawe[88], I. Dawson[139], R. K. Daya-Ishmukhametova[86], K. De[8], R. de Asmundis[104a], A. De Benedetti[113], S. De Castro[20a,20b], S. De Cecco[80], N. De Groot[106], P. de Jong[107], H. De la Torre[82], F. De Lorenzi[64], D. De Pedis[132a], A. De Salvo[132a], U. De Sanctis[149], A. De Santo[149], J. B. De Vivie De Regie[117], W. J. Dearnaley[72], R. Debbe[25], C. Debenedetti[137], D. V. Dedovich[65], I. Deigaard[107], J. Del Peso[82], T. Del Prete[124a,124b], D. Delgove[117], F. Deliot[136], C. M. Delitzsch[49], M. Deliyergiyev[75], A. Dell'Acqua[30], L. Dell'Asta[22], M. Dell'Orso[124a,124b], M. Della Pietra[104a,j], D. della Volpe[49], M. Delmastro[5], P. A. Delsart[55], C. Deluca[107], D. A. DeMarco[158], S. Demers[176], M. Demichev[65], A. Demilly[80], S. P. Denisov[130], D. Derendarz[39], J. E. Derkaoui[135d], F. Derue[80], P. Dervan[74], K. Desch[21], C. Deterre[42], P. O. Deviveiros[30], A. Dewhurst[131], S. Dhaliwal[23], A. Di Ciaccio[133a,133b], L. Di Ciaccio[5], A. Di Domenico[132a,132b], C. Di Donato[104a,104b], A. Di Girolamo[30], B. Di Girolamo[30], A. Di Mattia[152], B. Di Micco[134a,134b], R. Di Nardo[47], A. Di Simone[48], R. Di Sipio[158], D. Di Valentino[29], C. Diaconu[85], M. Diamond[158], F. A. Dias[46], M. A. Diaz[32a], E. B. Diehl[89], J. Dietrich[16], S. Diglio[85], A. Dimitrievska[13], J. Dingfelder[21], P. Dita[26a], S. Dita[26a], F. Dittus[30], F. Djama[85], T. Djobava[51b], J. I. Djuvsland[58a], M. A. B. do Vale[24c], D. Dobos[30], M. Dobre[26a], C. Doglioni[81], T. Dohmae[155], J. Dolejsi[129], Z. Dolezal[129], B. A. Dolgoshein[98,*], M. Donadelli[24d], S. Donati[124a,124b], P. Dondero[121a,121b], J. Donini[34], J. Dopke[131], A. Doria[104a], M. T. Dova[71], A. T. Doyle[53], E. Drechsler[54], M. Dris[10], E. Dubreuil[34], E. Duchovni[172],

G. Duckeck[100], O. A. Ducu[26a,85], D. Duda[107], A. Dudarev[30], L. Duflot[117], L. Duguid[77], M. Dührssen[30], M. Dunford[58a], H. Duran Yildiz[4a], M. Düren[52], A. Durglishvili[51b], D. Duschinger[44], M. Dyndal[38a], C. Eckardt[42], K. M. Ecker[101], R. C. Edgar[89], W. Edson[2], N. C. Edwards[46], W. Ehrenfeld[21], T. Eifert[30], G. Eigen[14], K. Einsweiler[15], T. Ekelof[166], M. El Kacimi[135c], M. Ellert[166], S. Elles[5], F. Ellinghaus[175], A. A. Elliot[169], N. Ellis[30], J. Elmsheuser[100], M. Elsing[30], D. Emeliyanov[131], Y. Enari[155], O. C. Endner[83], M. Endo[118], J. Erdmann[43], A. Ereditato[17], G. Ernis[175], J. Ernst[2], M. Ernst[25], S. Errede[165], E. Ertel[83], M. Escalier[117], H. Esch[43], C. Escobar[125], B. Esposito[47], A. I. Etienvre[136], E. Etzion[153], H. Evans[61], A. Ezhilov[123], L. Fabbri[20a,20b], G. Facini[31], R. M. Fakhrutdinov[130], S. Falciano[132a], R. J. Falla[78], J. Faltova[129], Y. Fang[33a], M. Fanti[91a,91b], A. Farbin[8], A. Farilla[134a], T. Farooque[12], S. Farrell[15], S. M. Farrington[170], P. Farthouat[30], F. Fassi[135e], P. Fassnacht[30], D. Fassouliotis[9], M. Faucci Giannelli[77], A. Favareto[50a,50b], L. Fayard[117], P. Federic[144a], O. L. Fedin[123,m], W. Fedorko[168], S. Feigl[30], L. Feligioni[85], C. Feng[33d], E. J. Feng[6], H. Feng[89], A. B. Fenyuk[130], L. Feremenga[8], P. Fernandez Martinez[167], S. Fernandez Perez[30], J. Ferrando[53], A. Ferrari[166], P. Ferrari[107], R. Ferrari[121a], D. E. Ferreira de Lima[53], A. Ferrer[167], D. Ferrere[49], C. Ferretti[89], A. Ferretto Parodi[50a,50b], M. Fiascaris[31], F. Fiedler[83], A. Filipčič[75], M. Filipuzzi[42], F. Filthaut[106], M. Fincke-Keeler[169], K. D. Finelli[150], M. C. N. Fiolhais[126a,126c], L. Fiorini[167], A. Firan[40], A. Fischer[2], C. Fischer[12], J. Fischer[175], W. C. Fisher[90], E. A. Fitzgerald[23], N. Flaschel[42], I. Fleck[141], P. Fleischmann[89], S. Fleischmann[175], G. T. Fletcher[139], G. Fletcher[76], R. R. M. Fletcher[122], T. Flick[175], A. Floderus[81], L. R. Flores Castillo[60a], M. J. Flowerdew[101], A. Formica[136], A. Forti[84], D. Fournier[117], H. Fox[72], S. Fracchia[12], P. Francavilla[80], M. Franchini[20a,20b], D. Francis[30], L. Franconi[119], M. Franklin[57], M. Frate[163], M. Fraternali[121a,121b], D. Freeborn[78], S. T. French[28], F. Friedrich[44], D. Froidevaux[30], J. A. Frost[120], C. Fukunaga[156], E. Fullana Torregrosa[83], B. G. Fulsom[143], T. Fusayasu[102], J. Fuster[167], C. Gabaldon[55], O. Gabizon[175], A. Gabrielli[20a,20b], A. Gabrielli[132a,132b], G. P. Gach[38a], S. Gadatsch[30], S. Gadomski[49], G. Gagliardi[50a,50b], P. Gagnon[61], C. Galea[106], B. Galhardo[126a,126c], E. J. Gallas[120], B. J. Gallop[131], P. Gallus[128], G. Galster[36], K. K. Gan[111], J. Gao[33b,85], Y. Gao[46], Y. S. Gao[143,e], F. M. Garay Walls[46], F. Garberson[176], C. García[167], J. E. García Navarro[167], M. Garcia-Sciveres[15], R. W. Gardner[31], N. Garelli[143], V. Garonne[119], C. Gatti[47], A. Gaudiello[50a,50b], G. Gaudio[121a], B. Gaur[141], L. Gauthier[95], P. Gauzzi[132a,132b], I. L. Gavrilenko[96], C. Gay[168], G. Gaycken[21], E. N. Gazis[10], P. Ge[33d], Z. Gecse[168], C. N. P. Gee[131], Ch. Geich-Gimbel[21], M. P. Geisler[58a], C. Gemme[50a], M. H. Genest[55], S. Gentile[132a,132b], M. George[54], S. George[77], D. Gerbaudo[163], A. Gershon[153], S. Ghasemi[141], H. Ghazlane[135b], B. Giacobbe[20a], S. Giagu[132a,132b], V. Giangiobbe[12], P. Giannetti[124a,124b], B. Gibbard[25], S. M. Gibson[77], M. Gilchriese[15], T. P. S. Gillam[28], D. Gillberg[30], G. Gilles[34], D. M. Gingrich[3,d], N. Giokaris[9], M. P. Giordani[164a,164c], F. M. Giorgi[20a], F. M. Giorgi[16], P. F. Giraud[136], P. Giromini[47], D. Giugni[91a], C. Giuliani[48], M. Giulini[58b], B. K. Gjelsten[119], S. Gkaitatzis[154], I. Gkialas[154], E. L. Gkougkousis[117], L. K. Gladilin[99], C. Glasman[82], J. Glatzer[30], P. C. F. Glaysher[46], A. Glazov[42], M. Goblirsch-Kolb[101], J. R. Goddard[76], J. Godlewski[39], S. Goldfarb[89], T. Golling[49], D. Golubkov[130], A. Gomes[126a,126b,126d], R. Gonçalo[126a], J. Goncalves Pinto Firmino Da Costa[136], L. Gonella[21], S. González de la Hoz[167], G. Gonzalez Parra[12], S. Gonzalez-Sevilla[49], L. Goossens[30], P. A. Gorbounov[97], H. A. Gordon[25], I. Gorelov[105], B. Gorini[30], E. Gorini[73a,73b], A. Gorišek[75], E. Gornicki[39], A. T. Goshaw[45], C. Gössling[43], M. I. Gostkin[65], D. Goujdami[135c], A. G. Goussiou[138], N. Govender[145b], E. Gozani[152], H. M. X. Grabas[137], L. Graber[54], I. Grabowska-Bold[38a], P. O. J. Gradin[166], P. Grafström[20a,20b], K-J. Grahn[42], J. Gramling[49], E. Gramstad[119], S. Grancagnolo[16], V. Gratchev[123], H. M. Gray[30], E. Graziani[134a], Z. D. Greenwood[79,n], K. Gregersen[78], I. M. Gregor[42], P. Grenier[143], J. Griffiths[8], A. A. Grillo[137], K. Grimm[72], S. Grinstein[12,o], Ph. Gris[34], J.-F. Grivaz[117], J. P. Grohs[44], A. Grohsjean[42], E. Gross[172], J. Grosse-Knetter[54], G. C. Grossi[79], Z. J. Grout[149], L. Guan[89], J. Guenther[128], F. Guescini[49], D. Guest[176], O. Gueta[153], E. Guido[50a,50b], T. Guillemin[117], S. Guindon[2], U. Gul[53], C. Gumpert[44], J. Guo[33e], Y. Guo[33b], S. Gupta[120], G. Gustavino[132a,132b], P. Gutierrez[113], N. G. Gutierrez Ortiz[78], C. Gutschow[44], C. Guyot[136], C. Gwenlan[120], C. B. Gwilliam[74], A. Haas[110], C. Haber[15], H. K. Hadavand[8], N. Haddad[135e], P. Haefner[21], S. Hageböck[21], Z. Hajduk[39], H. Hakobyan[177], M. Haleem[42], J. Haley[114], D. Hall[120], G. Halladjian[90], G. D. Hallewell[85], K. Hamacher[175], P. Hamal[115], K. Hamano[169], A. Hamilton[145a], G. N. Hamity[139], P. G. Hamnett[42], L. Han[33b], K. Hanagaki[66,p], K. Hanawa[155], M. Hance[15], P. Hanke[58a], R. Hanna[136], J. B. Hansen[36], J. D. Hansen[36], M. C. Hansen[21], P. H. Hansen[36], K. Hara[160], A. S. Hard[173], T. Harenberg[175], F. Hariri[117], S. Harkusha[92], R. D. Harrington[46], P. F. Harrison[170], F. Hartjes[107], M. Hasegawa[67], Y. Hasegawa[140], A. Hasib[113], S. Hassani[136], S. Haug[17], R. Hauser[90], L. Hauswald[44], M. Havranek[127], C. M. Hawkes[18], R. J. Hawkings[30], A. D. Hawkins[81], T. Hayashi[160], D. Hayden[90], C. P. Hays[120], J. M. Hays[76], H. S. Hayward[74], S. J. Haywood[131], S. J. Head[18], T. Heck[83], V. Hedberg[81], L. Heelan[8], S. Heim[122], T. Heim[175], B. Heinemann[15], L. Heinrich[110], J. Hejbal[127], L. Helary[22], S. Hellman[146a,146b], D. Hellmich[21], C. Helsens[12], J. Henderson[120], R. C. W. Henderson[72], Y. Heng[173], C. Hengler[42], S. Henkelmann[168], A. Henrichs[176], A. M. Henriques Correia[30], S. Henrot-Versille[117], G. H. Herbert[16], Y. Hernández Jiménez[167], R. Herrberg-Schubert[16], G. Herten[48], R. Hertenberger[100], L. Hervas[30], G. G. Hesketh[78], N. P. Hessey[107], J. W. Hetherly[40], R. Hickling[76], E. Higón-Rodriguez[167], E. Hill[169], J. C. Hill[28], K. H. Hiller[42], S. J. Hillier[18], I. Hinchliffe[15], E. Hines[122], R. R. Hinman[15], M. Hirose[157], D. Hirschbuehl[175],

J. Hobbs[148], N. Hod[107], M. C. Hodgkinson[139], P. Hodgson[139], A. Hoecker[30], M. R. Hoeferkamp[105], F. Hoenig[100], M. Hohlfeld[83], D. Hohn[21], T. R. Holmes[15], M. Homann[43], T. M. Hong[125], L. Hooft van Huysduynen[110], W. H. Hopkins[116], Y. Horii[103], A. J. Horton[142], J-Y. Hostachy[55], S. Hou[151], A. Hoummada[135a], J. Howard[120], J. Howarth[42], M. Hrabovsky[115], I. Hristova[16], J. Hrivnac[117], T. Hryn'ova[5], A. Hrynevich[93], C. Hsu[145c], P. J. Hsu[151,q], S.-C. Hsu[138], D. Hu[35], Q. Hu[33b], X. Hu[89], Y. Huang[42], Z. Hubacek[128], F. Hubaut[85], F. Huegging[21], T. B. Huffman[120], E. W. Hughes[35], G. Hughes[72], M. Huhtinen[30], T. A. Hülsing[83], N. Huseynov[65,b], J. Huston[90], J. Huth[57], G. Iacobucci[49], G. Iakovidis[25], I. Ibragimov[141], L. Iconomidou-Fayard[117], E. Ideal[176], Z. Idrissi[135e], P. Iengo[30], O. Igonkina[107], T. Iizawa[171], Y. Ikegami[66], K. Ikematsu[141], M. Ikeno[66], Y. Ilchenko[31,r], D. Iliadis[154], N. Ilic[143], T. Ince[101], G. Introzzi[121a,121b], P. Ioannou[9], M. Iodice[134a], K. Iordanidou[35], V. Ippolito[57], A. Irles Quiles[167], C. Isaksson[166], M. Ishino[68], M. Ishitsuka[157], R. Ishmukhametov[111], C. Issever[120], S. Istin[19a], J. M. Iturbe Ponce[84], R. Iuppa[133a,133b], J. Ivarsson[81], W. Iwanski[39], H. Iwasaki[66], J. M. Izen[41], V. Izzo[104a], S. Jabbar[3], B. Jackson[122], M. Jackson[74], P. Jackson[1], M. R. Jaekel[30], V. Jain[2], K. Jakobs[48], S. Jakobsen[30], T. Jakoubek[127], J. Jakubek[128], D. O. Jamin[114], D. K. Jana[79], E. Jansen[78], R. Jansky[62], J. Janssen[21], M. Janus[54], G. Jarlskog[81], N. Javadov[65,b], T. Javůrek[48], L. Jeanty[15], J. Jejelava[51a,s], G.-Y. Jeng[150], D. Jennens[88], P. Jenni[48,t], J. Jentzsch[43], C. Jeske[170], S. Jézéquel[5], H. Ji[173], J. Jia[148], Y. Jiang[33b], S. Jiggins[78], J. Jimenez Pena[167], S. Jin[33a], A. Jinaru[26a], O. Jinnouchi[157], M. D. Joergensen[36], P. Johansson[139], K. A. Johns[7], K. Jon-And[146a,146b], G. Jones[170], R. W. L. Jones[72], T. J. Jones[74], J. Jongmanns[58a], P. M. Jorge[126a,126b], K. D. Joshi[84], J. Jovicevic[159a], X. Ju[173], C. A. Jung[43], P. Jussel[62], A. Juste Rozas[12,o], M. Kaci[167], A. Kaczmarska[39], M. Kado[117], H. Kagan[111], M. Kagan[143], S. J. Kahn[85], E. Kajomovitz[45], C. W. Kalderon[120], S. Kama[40], A. Kamenshchikov[130], N. Kanaya[155], S. Kaneti[28], V. A. Kantserov[98], J. Kanzaki[66], B. Kaplan[110], L. S. Kaplan[173], A. Kapliy[31], D. Kar[145c], K. Karakostas[10], A. Karamaoun[3], N. Karastathis[10,107], M. J. Kareem[54], E. Karentzos[10], M. Karnevskiy[83], S. N. Karpov[65], Z. M. Karpova[65], K. Karthik[110], V. Kartvelishvili[72], A. N. Karyukhin[130], L. Kashif[173], R. D. Kass[111], A. Kastanas[14], Y. Kataoka[155], C. Kato[155], A. Katre[49], J. Katzy[42], K. Kawagoe[70], T. Kawamoto[155], G. Kawamura[54], S. Kazama[155], V. F. Kazanin[109,c], R. Keeler[169], R. Kehoe[40], J. S. Keller[42], J. J. Kempster[77], H. Keoshkerian[84], O. Kepka[127], B. P. Kerševan[75], S. Kersten[175], R. A. Keyes[87], F. Khalil-zada[11], H. Khandanyan[146a,146b], A. Khanov[114], A. G. Kharlamov[109,c], T. J. Khoo[28], V. Khovanskiy[97], E. Khramov[65], J. Khubua[51b,u], S. Kido[67], H. Y. Kim[8], S. H. Kim[160], Y. K. Kim[31], N. Kimura[154], O. M. Kind[16], B. T. King[74], M. King[167], S. B. King[168], J. Kirk[131], A. E. Kiryunin[101], T. Kishimoto[67], D. Kisielewska[38a], F. Kiss[48], K. Kiuchi[160], O. Kivernyk[136], E. Kladiva[144b], M. H. Klein[35], M. Klein[74], U. Klein[74], K. Kleinknecht[83], P. Klimek[146a,146b], A. Klimentov[25], R. Klingenberg[43], J. A. Klinger[139], T. Klioutchnikova[30], E.-E. Kluge[58a], P. Kluit[107], S. Kluth[101], J. Knapik[39], E. Kneringer[62], E. B. F. G. Knoops[85], A. Knue[53], A. Kobayashi[155], D. Kobayashi[157], T. Kobayashi[155], M. Kobel[44], M. Kocian[143], P. Kodys[129], T. Koffas[29], E. Koffeman[107], L. A. Kogan[120], S. Kohlmann[175], Z. Kohout[128], T. Kohriki[66], T. Koi[143], H. Kolanoski[16], I. Koletsou[5], A. A. Komar[96,*], Y. Komori[155], T. Kondo[66], N. Kondrashova[42], K. Köneke[48], A. C. König[106], T. Kono[66], R. Konoplich[110,v], N. Konstantinidis[78], R. Kopeliansky[152], S. Koperny[38a], L. Köpke[83], A. K. Kopp[48], K. Korcyl[39], K. Kordas[154], A. Korn[78], A. A. Korol[109,c], I. Korolkov[12], E. V. Korolkova[139], O. Kortner[101], S. Kortner[101], T. Kosek[129], V. V. Kostyukhin[21], V. M. Kotov[65], A. Kotwal[45], A. Kourkoumeli-Charalampidi[154], C. Kourkoumelis[9], V. Kouskoura[25], A. Koutsman[159a], R. Kowalewski[169], T. Z. Kowalski[38a], W. Kozanecki[136], A. S. Kozhin[130], V. A. Kramarenko[99], G. Kramberger[75], D. Krasnopevtsev[98], M. W. Krasny[80], A. Krasznahorkay[30], J. K. Kraus[21], A. Kravchenko[25], S. Kreiss[110], M. Kretz[58c], J. Kretzschmar[74], K. Kreutzfeldt[52], P. Krieger[158], K. Krizka[31], K. Kroeninger[43], H. Kroha[101], J. Kroll[122], J. Kroseberg[21], J. Krstic[13], U. Kruchonak[65], H. Krüger[21], N. Krumnack[64], A. Kruse[173], M. C. Kruse[45], M. Kruskal[22], T. Kubota[88], H. Kucuk[78], S. Kuday[4b], S. Kuehn[48], A. Kugel[58c], F. Kuger[174], A. Kuhl[137], T. Kuhl[42], V. Kukhtin[65], R. Kukla[136], Y. Kulchitsky[92], S. Kuleshov[32b], M. Kuna[132a,132b], T. Kunigo[68], A. Kupco[127], H. Kurashige[67], Y. A. Kurochkin[92], V. Kus[127], E. S. Kuwertz[169], M. Kuze[157], J. Kvita[115], T. Kwan[169], D. Kyriazopoulos[139], A. La Rosa[137], J. L. La Rosa Navarro[24d], L. La Rotonda[37a,37b], C. Lacasta[167], F. Lacava[132a,132b], J. Lacey[29], H. Lacker[16], D. Lacour[80], V. R. Lacuesta[167], E. Ladygin[65], R. Lafaye[5], B. Laforge[80], T. Lagouri[176], S. Lai[54], L. Lambourne[78], S. Lammers[61], C. L. Lampen[7], W. Lampl[7], E. Lançon[136], U. Landgraf[48], M. P. J. Landon[76], V. S. Lang[58a], J. C. Lange[12], A. J. Lankford[163], F. Lanni[25], K. Lantzsch[21], A. Lanza[121a], S. Laplace[80], C. Lapoire[30], J. F. Laporte[136], T. Lari[91a], F. Lasagni Manghi[20a,20b], M. Lassnig[30], P. Laurelli[47], W. Lavrijsen[15], A. T. Law[137], P. Laycock[74], T. Lazovich[57], O. Le Dortz[80], E. Le Guirriec[85], E. Le Menedeu[12], M. LeBlanc[169], T. LeCompte[6], F. Ledroit-Guillon[55], C. A. Lee[145b], S. C. Lee[151], L. Lee[1], G. Lefebvre[80], M. Lefebvre[169], F. Legger[100], C. Leggett[15], A. Lehan[74], G. Lehmann Miotto[30], X. Lei[7], W. A. Leight[29], A. Leisos[154,w], A. G. Leister[176], M. A. L. Leite[24d], R. Leitner[129], D. Lellouch[172], B. Lemmer[54], K. J. C. Leney[78], T. Lenz[21], B. Lenzi[30], R. Leone[7], S. Leone[124a,124b], C. Leonidopoulos[46], S. Leontsinis[10], C. Leroy[95], C. G. Lester[28], M. Levchenko[123], J. Levêque[5], D. Levin[89], L. J. Levinson[172], M. Levy[18], A. Lewis[120], A. M. Leyko[21], M. Leyton[41], B. Li[33b,x], H. Li[148], H. L. Li[31], L. Li[45], L. Li[33e], S. Li[45], X. Li[84], Y. Li[33c,y], Z. Liang[137], H. Liao[34], B. Liberti[133a], A. Liblong[158], P. Lichard[30], K. Lie[165], J. Liebal[21],

W. Liebig[14], C. Limbach[21], A. Limosani[150], S. C. Lin[151,z], T. H. Lin[83], F. Linde[107], B. E. Lindquist[148], J. T. Linnemann[90], E. Lipeles[122], A. Lipniacka[14], M. Lisovyi[58b], T. M. Liss[165], D. Lissauer[25], A. Lister[168], A. M. Litke[137], B. Liu[151,aa], D. Liu[151], H. Liu[89], J. Liu[85], J. B. Liu[33b], K. Liu[85], L. Liu[165], M. Liu[45], M. Liu[33b], Y. Liu[33b], M. Livan[121a,121b], A. Lleres[55], J. Llorente Merino[82], S. L. Lloyd[76], F. Lo Sterzo[151], E. Lobodzinska[42], P. Loch[7], W. S. Lockman[137], F. K. Loebinger[84], A. E. Loevschall-Jensen[36], A. Loginov[176], T. Lohse[16], K. Lohwasser[42], M. Lokajicek[127], B. A. Long[22], J. D. Long[89], R. E. Long[72], K. A. Looper[111], L. Lopes[126a], D. Lopez Mateos[57], B. Lopez Paredes[139], I. Lopez Paz[12], J. Lorenz[100], N. Lorenzo Martinez[61], M. Losada[162], P. Loscutoff[15], P. J. Lösel[100], X. Lou[33a], A. Lounis[117], J. Love[6], P. A. Love[72], N. Lu[89], H. J. Lubatti[138], C. Luci[132a,132b], A. Lucotte[55], F. Luehring[61], W. Lukas[62], L. Luminari[132a], O. Lundberg[146a,146b], B. Lund-Jensen[147], D. Lynn[25], R. Lysak[127], E. Lytken[81], H. Ma[25], L. L. Ma[33d], G. Maccarrone[47], A. Macchiolo[101], C. M. Macdonald[139], B. Maček[75], J. Machado Miguens[122,126b], D. Macina[30], D. Madaffari[85], R. Madar[34], H. J. Maddocks[72], W. F. Mader[44], A. Madsen[166], J. Maeda[67], S. Maeland[14], T. Maeno[25], A. Maevskiy[99], E. Magradze[54], K. Mahboubi[48], J. Mahlstedt[107], C. Maiani[136], C. Maidantchik[24a], A. A. Maier[101], T. Maier[100], A. Maio[126a,126b,126d], S. Majewski[116], Y. Makida[66], N. Makovec[117], B. Malaescu[80], Pa. Malecki[39], V. P. Maleev[123], F. Malek[55], U. Mallik[63], D. Malon[6], C. Malone[143], S. Maltezos[10], V. M. Malyshev[109], S. Malyukov[30], J. Mamuzic[42], G. Mancini[47], B. Mandelli[30], L. Mandelli[91a], I. Mandić[75], R. Mandrysch[63], J. Maneira[126a,126b], A. Manfredini[101], L. Manhaes de Andrade Filho[24b], J. Manjarres Ramos[159b], A. Mann[100], A. Manousakis-Katsikakis[9], B. Mansoulie[136], R. Mantifel[87], M. Mantoani[54], L. Mapelli[30], L. March[145c], G. Marchiori[80], M. Marcisovsky[127], C. P. Marino[169], M. Marjanovic[13], D. E. Marley[89], F. Marroquim[24a], S. P. Marsden[84], Z. Marshall[15], L. F. Marti[17], S. Marti-Garcia[167], B. Martin[90], T. A. Martin[170], V. J. Martin[46], B. Martin dit Latour[14], M. Martinez[12,o], S. Martin-Haugh[131], V. S. Martoiu[26a], A. C. Martyniuk[78], M. Marx[138], F. Marzano[132a], A. Marzin[30], L. Masetti[83], T. Mashimo[155], R. Mashinistov[96], J. Masik[84], A. L. Maslennikov[109,c], I. Massa[20a,20b], L. Massa[20a,20b], N. Massol[5], P. Mastrandrea[148], A. Mastroberardino[37a,37b], T. Masubuchi[155], P. Mättig[175], J. Mattmann[83], J. Maurer[26a], S. J. Maxfield[74], D. A. Maximov[109,c], R. Mazini[151], S. M. Mazza[91a,91b], L. Mazzaferro[133a,133b], G. Mc Goldrick[158], S. P. Mc Kee[89], A. McCarn[89], R. L. McCarthy[148], T. G. McCarthy[29], N. A. McCubbin[131], K. W. McFarlane[56,*], J. A. Mcfayden[78], G. Mchedlidze[54], S. J. McMahon[131], R. A. McPherson[169,k], M. Medinnis[42], S. Meehan[145a], S. Mehlhase[100], A. Mehta[74], K. Meier[58a], C. Meineck[100], B. Meirose[41], B. R. Mellado Garcia[145c], F. Meloni[17], A. Mengarelli[20a,20b], S. Menke[101], E. Meoni[161], K. M. Mercurio[57], S. Mergelmeyer[21], P. Mermod[49], L. Merola[104a,104b], C. Meroni[91a], F. S. Merritt[31], A. Messina[132a,132b], J. Metcalfe[25], A. S. Mete[163], C. Meyer[83], C. Meyer[122], J-P. Meyer[136], J. Meyer[107], H. Meyer Zu Theenhausen[58a], R. P. Middleton[131], S. Miglioranzi[164a,164c], L. Mijović[21], G. Mikenberg[172], M. Mikestikova[127], M. Mikuž[75], M. Milesi[88], A. Milic[30], D. W. Miller[31], C. Mills[46], A. Milov[172], D. A. Milstead[146a,146b], A. A. Minaenko[130], Y. Minami[155], I. A. Minashvili[65], A. I. Mincer[110], B. Mindur[38a], M. Mineev[65], Y. Ming[173], L. M. Mir[12], T. Mitani[171], J. Mitrevski[100], V. A. Mitsou[167], A. Miucci[49], P. S. Miyagawa[139], J. U. Mjörnmark[81], T. Moa[146a,146b], K. Mochizuki[85], S. Mohapatra[35], W. Mohr[48], S. Molander[146a,146b], R. Moles-Valls[21], K. Mönig[42], C. Monini[55], J. Monk[36], E. Monnier[85], J. Montejo Berlingen[12], F. Monticelli[71], S. Monzani[132a,132b], R. W. Moore[3], N. Morange[117], D. Moreno[162], M. Moreno Llácer[54], P. Morettini[50a], D. Mori[142], M. Morii[57], M. Morinaga[155], V. Morisbak[119], S. Moritz[83], A. K. Morley[150], G. Mornacchi[30], J. D. Morris[76], S. S. Mortensen[36], A. Morton[53], L. Morvaj[103], M. Mosidze[51b], J. Moss[143], K. Motohashi[157], R. Mount[143], E. Mountricha[25], S. V. Mouraviev[96,*], E. J. W. Moyse[86], S. Muanza[85], R. D. Mudd[18], F. Mueller[101], J. Mueller[125], R. S. P. Mueller[100], T. Mueller[28], D. Muenstermann[49], P. Mullen[53], G. A. Mullier[17], J. A. Murillo Quijada[18], W. J. Murray[131,170], H. Musheghyan[54], E. Musto[152], A. G. Myagkov[130,ab], M. Myska[128], B. P. Nachman[143], O. Nackenhorst[54], J. Nadal[54], K. Nagai[120], R. Nagai[157], Y. Nagai[85], K. Nagano[66], A. Nagarkar[111], Y. Nagasaka[59], K. Nagata[160], M. Nagel[101], E. Nagy[85], A. M. Nairz[30], Y. Nakahama[30], K. Nakamura[66], T. Nakamura[155], I. Nakano[112], H. Namasivayam[41], R. F. Naranjo Garcia[42], R. Narayan[31], D. I. Narrias Villar[58a], T. Naumann[42], G. Navarro[162], R. Nayyar[7], H. A. Neal[89], P. Yu. Nechaeva[96], T. J. Neep[84], P. D. Nef[143], A. Negri[121a,121b], M. Negrini[20a], S. Nektarijevic[106], C. Nellist[117], A. Nelson[163], S. Nemecek[127], P. Nemethy[110], A. A. Nepomuceno[24a], M. Nessi[30,ac], M. S. Neubauer[165], M. Neumann[175], R. M. Neves[110], P. Nevski[25], P. R. Newman[18], D. H. Nguyen[6], R. B. Nickerson[120], R. Nicolaidou[136], B. Nicquevert[30], J. Nielsen[137], N. Nikiforou[35], A. Nikiforov[16], V. Nikolaenko[130,ab], I. Nikolic-Audit[80], K. Nikolopoulos[18], J. K. Nilsen[119], P. Nilsson[25], Y. Ninomiya[155], A. Nisati[132a], R. Nisius[101], T. Nobe[155], M. Nomachi[118], I. Nomidis[29], T. Nooney[76], S. Norberg[113], M. Nordberg[30], O. Novgorodova[44], S. Nowak[101], M. Nozaki[66], L. Nozka[115], K. Ntekas[10], G. Nunes Hanninger[88], T. Nunnemann[100], E. Nurse[78], F. Nuti[88], B. J. O'Brien[46], F. O'grady[7], D. C. O'Neil[142], V. O'Shea[53], F. G. Oakham[29,d], H. Oberlack[101], T. Obermann[21], J. Ocariz[80], A. Ochi[67], I. Ochoa[78], J. P. Ochoa-Ricoux[32a], S. Oda[70], S. Odaka[66], H. Ogren[61], A. Oh[84], S. H. Oh[45], C. C. Ohm[15], H. Ohman[166], H. Oide[30], W. Okamura[118], H. Okawa[160], Y. Okumura[31], T. Okuyama[66], A. Olariu[26a], S. A. Olivares Pino[46], D. Oliveira Damazio[25], E. Oliver Garcia[167], A. Olszewski[39], J. Olszowska[39], A. Onofre[126a,126e], P. U. E. Onyisi[31,r], C. J. Oram[159a], M. J. Oreglia[31], Y. Oren[153], D. Orestano[134a,134b], N. Orlando[154],

C. Oropeza Barrera[53], R. S. Orr[158], B. Osculati[50a,50b], R. Ospanov[84], G. Otero y Garzon[27], H. Otono[70], M. Ouchrif[135d], F. Ould-Saada[119], A. Ouraou[136], K. P. Oussoren[107], Q. Ouyang[33a], A. Ovcharova[15], M. Owen[53], R. E. Owen[18], V. E. Ozcan[19a], N. Ozturk[8], K. Pachal[142], A. Pacheco Pages[12], C. Padilla Aranda[12], M. Pagáčová[48], S. Pagan Griso[15], E. Paganis[139], F. Paige[25], P. Pais[86], K. Pajchel[119], G. Palacino[159b], S. Palestini[30], M. Palka[38b], D. Pallin[34], A. Palma[126a,126b], Y. B. Pan[173], E. Panagiotopoulou[10], C. E. Pandini[80], J. G. Panduro Vazquez[77], P. Pani[146a,146b], S. Panitkin[25], D. Pantea[26a], L. Paolozzi[49], Th. D. Papadopoulou[10], K. Papageorgiou[154], A. Paramonov[6], D. Paredes Hernandez[154], M. A. Parker[28], K. A. Parker[139], F. Parodi[50a,50b], J. A. Parsons[35], U. Parzefall[48], E. Pasqualucci[132a], S. Passaggio[50a], F. Pastore[134a,134b,*], Fr. Pastore[77], G. Pásztor[29], S. Pataraia[175], N. D. Patel[150], J. R. Pater[84], T. Pauly[30], J. Pearce[169], B. Pearson[113], L. E. Pedersen[36], M. Pedersen[119], S. Pedraza Lopez[167], R. Pedro[126a,126b], S. V. Peleganchuk[109,c], D. Pelikan[166], O. Penc[127], C. Peng[33a], H. Peng[33b], B. Penning[31], J. Penwell[61], D. V. Perepelitsa[25], E. Perez Codina[159a], M. T. Pérez García-Estañ[167], L. Perini[91a,91b], H. Pernegger[30], S. Perrella[104a,104b], R. Peschke[42], V. D. Peshekhonov[65], K. Peters[30], R. F. Y. Peters[84], B. A. Petersen[30], T. C. Petersen[36], E. Petit[42], A. Petridis[1], C. Petridou[154], P. Petroff[117], E. Petrolo[132a], F. Petrucci[134a,134b], N. E. Pettersson[157], R. Pezoa[32b], P. W. Phillips[131], G. Piacquadio[143], E. Pianori[170], A. Picazio[49], E. Piccaro[76], M. Piccinini[20a,20b], M. A. Pickering[120], R. Piegaia[27], D. T. Pignotti[111], J. E. Pilcher[31], A. D. Pilkington[84], J. Pina[126a,126b,126d], M. Pinamonti[164a,164c,ad], J. L. Pinfold[3], A. Pingel[36], S. Pires[80], H. Pirumov[42], M. Pitt[172], C. Pizio[91a,91b], L. Plazak[144a], M.-A. Pleier[25], V. Pleskot[129], E. Plotnikova[65], P. Plucinski[146a,146b], D. Pluth[64], R. Poettgen[146a,146b], L. Poggioli[117], D. Pohl[21], G. Polesello[121a], A. Poley[42], A. Policicchio[37a,37b], R. Polifka[158], A. Polini[20a], C. S. Pollard[53], V. Polychronakos[25], K. Pommès[30], L. Pontecorvo[132a], B. G. Pope[90], G. A. Popeneciu[26b], D. S. Popovic[13], A. Poppleton[30], S. Pospisil[128], K. Potamianos[15], I. N. Potrap[65], C. J. Potter[149], C. T. Potter[116], G. Poulard[30], J. Poveda[30], V. Pozdnyakov[65], P. Pralavorio[85], A. Pranko[15], S. Prasad[30], S. Prell[64], D. Price[84], L. E. Price[6], M. Primavera[73a], S. Prince[87], M. Proissl[46], K. Prokofiev[60c], F. Prokoshin[32b], E. Protopapadaki[136], S. Protopopescu[25], J. Proudfoot[6], M. Przybycien[38a], E. Ptacek[116], D. Puddu[134a,134b], E. Pueschel[86], D. Puldon[148], M. Purohit[25,ae], P. Puzo[117], J. Qian[89], G. Qin[53], Y. Qin[84], A. Quadt[54], D. R. Quarrie[15], W. B. Quayle[164a,164b], M. Queitsch-Maitland[84], D. Quilty[53], S. Raddum[119], V. Radeka[25], V. Radescu[42], S. K. Radhakrishnan[148], P. Radloff[116], P. Rados[88], F. Ragusa[91a,91b], G. Rahal[178], S. Rajagopalan[25], M. Rammensee[30], C. Rangel-Smith[166], F. Rauscher[100], S. Rave[83], T. Ravenscroft[53], M. Raymond[30], A. L. Read[119], N. P. Readioff[74], D. M. Rebuzzi[121a,121b], A. Redelbach[174], G. Redlinger[25], R. Reece[137], K. Reeves[41], L. Rehnisch[16], J. Reichert[122], H. Reisin[27], M. Relich[163], C. Rembser[30], H. Ren[33a], A. Renaud[117], M. Rescigno[132a], S. Resconi[91a], O. L. Rezanova[109,c], P. Reznicek[129], R. Rezvani[95], R. Richter[101], S. Richter[78], E. Richter-Was[38b], O. Ricken[21], M. Ridel[80], P. Rieck[16], C. J. Riegel[175], J. Rieger[54], M. Rijssenbeek[148], A. Rimoldi[121a,121b], L. Rinaldi[20a], B. Ristić[49], E. Ritsch[30], I. Riu[12], F. Rizatdinova[114], E. Rizvi[76], C. Rizzi[12], S. H. Robertson[87,k], A. Robichaud-Veronneau[87], D. Robinson[28], J. E. M. Robinson[42], A. Robson[53], C. Roda[124a,124b], S. Roe[30], O. Røhne[119], S. Rolli[161], A. Romaniouk[98], M. Romano[20a,20b], S. M. Romano Saez[34], E. Romero Adam[167], N. Rompotis[138], M. Ronzani[48], L. Roos[80], E. Ros[167], S. Rosati[132a], K. Rosbach[48], P. Rose[137], P. L. Rosendahl[14], O. Rosenthal[141], V. Rossetti[146a,146b], E. Rossi[104a,104b], L. P. Rossi[50a], J. H. N. Rosten[28], R. Rosten[138], M. Rotaru[26a], I. Roth[172], J. Rothberg[138], D. Rousseau[117], C. R. Royon[136], A. Rozanov[85], Y. Rozen[152], X. Ruan[145c], F. Rubbo[143], I. Rubinskiy[42], V. I. Rud[99], C. Rudolph[44], M. S. Rudolph[158], F. Rühr[48], A. Ruiz-Martinez[30], Z. Rurikova[48], N. A. Rusakovich[65], A. Ruschke[100], H. L. Russell[138], J. P. Rutherfoord[7], N. Ruthmann[48], Y. F. Ryabov[123], M. Rybar[165], G. Rybkin[117], N. C. Ryder[120], A. F. Saavedra[150], G. Sabato[107], S. Sacerdoti[27], A. Saddique[3], H. F-W. Sadrozinski[137], R. Sadykov[65], F. Safai Tehrani[132a], M. Sahinsoy[58a], M. Saimpert[136], T. Saito[155], H. Sakamoto[155], Y. Sakurai[171], G. Salamanna[134a,134b], A. Salamon[133a], J. E. Salazar Loyola[32b], M. Saleem[113], D. Salek[107], P. H. Sales De Bruin[138], D. Salihagic[101], A. Salnikov[143], J. Salt[167], D. Salvatore[37a,37b], F. Salvatore[149], A. Salvucci[60a], A. Salzburger[30], D. Sammel[48], D. Sampsonidis[154], A. Sanchez[104a,104b], J. Sánchez[167], V. Sanchez Martinez[167], H. Sandaker[119], R. L. Sandbach[76], H. G. Sander[83], M. P. Sanders[100], M. Sandhoff[175], C. Sandoval[162], R. Sandstroem[101], D. P. C. Sankey[131], M. Sannino[50a,50b], A. Sansoni[47], C. Santoni[34], R. Santonico[133a,133b], H. Santos[126a], I. Santoyo Castillo[149], K. Sapp[125], A. Sapronov[65], J. G. Saraiva[126a,126d], B. Sarrazin[21], O. Sasaki[66], Y. Sasaki[155], K. Sato[160], G. Sauvage[5,*], E. Sauvan[5], G. Savage[77], P. Savard[158,d], C. Sawyer[131], L. Sawyer[79,n], J. Saxon[31], C. Sbarra[20a], A. Sbrizzi[20a,20b], T. Scanlon[78], D. A. Scannicchio[163], M. Scarcella[150], V. Scarfone[37a,37b], J. Schaarschmidt[172], P. Schacht[101], D. Schaefer[30], R. Schaefer[42], J. Schaeffer[83], S. Schaepe[21], S. Schaetzel[58b], U. Schäfer[83], A. C. Schaffer[117], D. Schaile[100], R. D. Schamberger[148], V. Scharf[58a], V. A. Schegelsky[123], D. Scheirich[129], M. Schernau[163], C. Schiavi[50a,50b], C. Schillo[48], M. Schioppa[37a,37b], S. Schlenker[30], K. Schmieden[30], C. Schmitt[83], S. Schmitt[58b], S. Schmitt[42], B. Schneider[159a], Y. J. Schnellbach[74], U. Schnoor[44], L. Schoeffel[136], A. Schoening[58b], B. D. Schoenrock[90], E. Schopf[21], A. L. S. Schorlemmer[54], M. Schott[83], D. Schouten[159a], J. Schovancova[8], S. Schramm[49], M. Schreyer[174], C. Schroeder[83], N. Schuh[83], M. J. Schultens[21], H.-C. Schultz-Coulon[58a], H. Schulz[16], M. Schumacher[48], B. A. Schumm[137], Ph. Schune[136], C. Schwanenberger[84], A. Schwartzman[143], T. A. Schwarz[89], Ph. Schwegler[101], H. Schweiger[84],

Ph. Schwemling[136], R. Schwienhorst[90], J. Schwindling[136], T. Schwindt[21], F. G. Sciacca[17], E. Scifo[117], G. Sciolla[23], F. Scuri[124a,124b], F. Scutti[21], J. Searcy[89], G. Sedov[42], E. Sedykh[123], P. Seema[21], S. C. Seidel[105], A. Seiden[137], F. Seifert[128], J. M. Seixas[24a], G. Sekhniaidze[104a], K. Sekhon[89], S. J. Sekula[40], D. M. Seliverstov[123,*], N. Semprini-Cesari[20a,20b], C. Serfon[30], L. Serin[117], L. Serkin[164a,164b], T. Serre[85], M. Sessa[134a,134b], R. Seuster[159a], H. Severini[113], T. Sfiligoj[75], F. Sforza[30], A. Sfyrla[30], E. Shabalina[54], M. Shamim[116], L. Y. Shan[33a], R. Shang[165], J. T. Shank[22], M. Shapiro[15], P. B. Shatalov[97], K. Shaw[164a,164b], S. M. Shaw[84], A. Shcherbakova[146a,146b], C. Y. Shehu[149], P. Sherwood[78], L. Shi[151,af], S. Shimizu[67], C. O. Shimmin[163], M. Shimojima[102], M. Shiyakova[65], A. Shmeleva[96], D. Shoaleh Saadi[95], M. J. Shochet[31], S. Shojaii[91a,91b], S. Shrestha[111], E. Shulga[98], M. A. Shupe[7], S. Shushkevich[42], P. Sicho[127], P. E. Sidebo[147], O. Sidiropoulou[174], D. Sidorov[114], A. Sidoti[20a,20b], F. Siegert[44], Dj. Sijacki[13], J. Silva[126a,126d], Y. Silver[153], S. B. Silverstein[146a], V. Simak[128], O. Simard[5], Lj. Simic[13], S. Simion[117], E. Simioni[83], B. Simmons[78], D. Simon[34], P. Sinervo[158], N. B. Sinev[116], M. Sioli[20a,20b], G. Siragusa[174], A. N. Sisakyan[65,*], S. Yu. Sivoklokov[99], J. Sjölin[146a,146b], T. B. Sjursen[14], M. B. Skinner[72], H. P. Skottowe[57], P. Skubic[113], M. Slater[18], T. Slavicek[128], M. Slawinska[107], K. Sliwa[161], V. Smakhtin[172], B. H. Smart[46], L. Smestad[14], S. Yu. Smirnov[98], Y. Smirnov[98], L. N. Smirnova[99,ag], O. Smirnova[81], M. N. K. Smith[35], R. W. Smith[35], M. Smizanska[72], K. Smolek[128], A. A. Snesarev[96], G. Snidero[76], S. Snyder[25], R. Sobie[169,k], F. Socher[44], A. Soffer[153], D. A. Soh[151,af], G. Sokhrannyi[75], C. A. Solans[30], M. Solar[128], J. Solc[128], E. Yu. Soldatov[98], U. Soldevila[167], A. A. Solodkov[130], A. Soloshenko[65], O. V. Solovyanov[130], V. Solovyev[123], P. Sommer[48], H. Y. Song[33b], N. Soni[1], A. Sood[15], A. Sopczak[128], B. Sopko[128], V. Sopko[128], V. Sorin[12], D. Sosa[58b], M. Sosebee[8], C. L. Sotiropoulou[124a,124b], R. Soualah[164a,164c], A. M. Soukharev[109,c], D. South[42], B. C. Sowden[77], S. Spagnolo[73a,73b], M. Spalla[124a,124b], M. Spangenberg[170], F. Spanò[77], W. R. Spearman[57], D. Sperlich[16], F. Spettel[101], R. Spighi[20a], G. Spigo[30], L. A. Spiller[88], M. Spousta[129], T. Spreitzer[158], R. D. St. Denis[53,*], S. Staerz[44], J. Stahlman[122], R. Stamen[58a], S. Stamm[16], E. Stanecka[39], C. Stanescu[134a], M. Stanescu-Bellu[42], M. M. Stanitzki[42], S. Stapnes[119], E. A. Starchenko[130], J. Stark[55], P. Staroba[127], P. Starovoitov[58a], R. Staszewski[39], P. Stavina[144a,*], P. Steinberg[25], B. Stelzer[142], H. J. Stelzer[30], O. Stelzer-Chilton[159a], H. Stenzel[52], G. A. Stewart[53], J. A. Stillings[21], M. C. Stockton[87], M. Stoebe[87], G. Stoicea[26a], P. Stolte[54], S. Stonjek[101], A. R. Stradling[8], A. Straessner[44], M. E. Stramaglia[17], J. Strandberg[147], S. Strandberg[146a,146b], A. Strandlie[119], E. Strauss[143], M. Strauss[113], P. Strizenec[144b], R. Ströhmer[174], D. M. Strom[116], R. Stroynowski[40], A. Strubig[106], S. A. Stucci[17], B. Stugu[14], N. A. Styles[42], D. Su[143], J. Su[125], R. Subramaniam[79], A. Succurro[12], Y. Sugaya[118], C. Suhr[108], M. Suk[128], V. V. Sulin[96], S. Sultansoy[4c], T. Sumida[68], S. Sun[57], X. Sun[33a], J. E. Sundermann[48], K. Suruliz[149], G. Susinno[37a,37b], M. R. Sutton[149], S. Suzuki[66], M. Svatos[127], M. Swiatlowski[143], I. Sykora[144a], T. Sykora[129], D. Ta[90], C. Taccini[134a,134b], K. Tackmann[42], J. Taenzer[158], A. Taffard[163], R. Tafirout[159a], N. Taiblum[153], H. Takai[25], R. Takashima[69], H. Takeda[67], T. Takeshita[140], Y. Takubo[66], M. Talby[85], A. A. Talyshev[109,c], J. Y. C. Tam[174], K. G. Tan[88], J. Tanaka[155], R. Tanaka[117], S. Tanaka[66], B. B. Tannenwald[111], N. Tannoury[21], S. Tapprogge[83], S. Tarem[152], F. Tarrade[29], G. F. Tartarelli[91a], P. Tas[129], M. Tasevsky[127], T. Tashiro[68], E. Tassi[37a,37b], A. Tavares Delgado[126a,126b], Y. Tayalati[135d], F. E. Taylor[94], G. N. Taylor[88], W. Taylor[159b], F. A. Teischinger[30], M. Teixeira Dias Castanheira[76], P. Teixeira-Dias[77], K. K. Temming[48], D. Temple[142], H. Ten Kate[30], P. K. Teng[151], J. J. Teoh[118], F. Tepel[175], S. Terada[66], K. Terashi[155], J. Terron[82], S. Terzo[101], M. Testa[47], R. J. Teuscher[158,k], T. Theveneaux-Pelzer[34], J. P. Thomas[18], J. Thomas-Wilsker[77], E. N. Thompson[35], P. D. Thompson[18], R. J. Thompson[84], A. S. Thompson[53], L. A. Thomsen[176], E. Thomson[122], M. Thomson[28], R. P. Thun[89,*], M. J. Tibbetts[15], R. E. Ticse Torres[85], V. O. Tikhomirov[96,ah], Yu. A. Tikhonov[109,c], S. Timoshenko[98], E. Tiouchichine[85], P. Tipton[176], S. Tisserant[85], K. Todome[157], T. Todorov[5,*], S. Todorova-Nova[129], J. Tojo[70], S. Tokár[144a], K. Tokushuku[66], K. Tollefson[90], E. Tolley[57], L. Tomlinson[84], M. Tomoto[103], L. Tompkins[143,ai], K. Toms[105], E. Torrence[116], H. Torres[142], E. Torró Pastor[138], J. Toth[85,aj], F. Touchard[85], D. R. Tovey[139], T. Trefzger[174], L. Tremblet[30], A. Tricoli[30], I. M. Trigger[159a], S. Trincaz-Duvoid[80], M. F. Tripiana[12], W. Trischuk[158], B. Trocmé[55], C. Troncon[91a], M. Trottier-McDonald[15], M. Trovatelli[169], P. True[90], L. Truong[164a,164c], M. Trzebinski[39], A. Trzupek[39], C. Tsarouchas[30], J. C-L. Tseng[120], P. V. Tsiareshka[92], D. Tsionou[154], G. Tsipolitis[10], N. Tsirintanis[9], S. Tsiskaridze[12], V. Tsiskaridze[48], E. G. Tskhadadze[51a], I. I. Tsukerman[97], V. Tsulaia[15], S. Tsuno[66], D. Tsybychev[148], A. Tudorache[26a], V. Tudorache[26a], A. N. Tuna[57], S. A. Tupputi[20a,20b], S. Turchikhin[99,ag], D. Turecek[128], R. Turra[91a,91b], A. J. Turvey[40], P. M. Tuts[35], A. Tykhonov[49], M. Tylmad[146a,146b], M. Tyndel[131], I. Ueda[155], R. Ueno[29], M. Ughetto[146a,146b], M. Ugland[14], F. Ukegawa[160], G. Unal[30], A. Undrus[25], G. Unel[163], F. C. Ungaro[48], Y. Unno[66], C. Unverdorben[100], J. Urban[144b], P. Urquijo[88], P. Urrejola[83], G. Usai[8], A. Usanova[62], L. Vacavant[85], V. Vacek[128], B. Vachon[87], C. Valderanis[83], N. Valencic[107], S. Valentinetti[20a,20b], A. Valero[167], L. Valery[12], S. Valkar[129], E. Valladolid Gallego[167], S. Vallecorsa[49], J. A. Valls Ferrer[167], W. Van Den Wollenberg[107], P. C. Van Der Deijl[107], R. van der Geer[107], H. van der Graaf[107], N. van Eldik[152], P. van Gemmeren[6], J. Van Nieuwkoop[142], I. van Vulpen[107], M. C. van Woerden[30], M. Vanadia[132a,132b], W. Vandelli[30], R. Vanguri[122], A. Vaniachine[6], F. Vannucci[80], G. Vardanyan[177], R. Vari[132a], E. W. Varnes[7], T. Varol[40], D. Varouchas[80], A. Vartapetian[8], K. E. Varvell[150], F. Vazeille[34], T. Vazquez Schroeder[87], J. Veatch[7], L. M. Veloce[158],

F. Veloso[126a,126c], T. Velz[21], S. Veneziano[132a], A. Ventura[73a,73b], D. Ventura[86], M. Venturi[169], N. Venturi[158], A. Venturini[23], V. Vercesi[121a], M. Verducci[132a,132b], W. Verkerke[107], J. C. Vermeulen[107], A. Vest[44], M. C. Vetterli[142,d], O. Viazlo[81], I. Vichou[165], T. Vickey[139], O. E. Vickey Boeriu[139], G. H. A. Viehhauser[120], S. Viel[15], R. Vigne[62], M. Villa[20a,20b], M. Villaplana Perez[91a,91b], E. Vilucchi[47], M. G. Vincter[29], V. B. Vinogradov[65], I. Vivarelli[149], F. Vives Vaque[3], S. Vlachos[10], D. Vladoiu[100], M. Vlasak[128], M. Vogel[32a], P. Vokac[128], G. Volpi[124a,124b], M. Volpi[88], H. von der Schmitt[101], H. von Radziewski[48], E. von Toerne[21], V. Vorobel[129], K. Vorobev[98], M. Vos[167], R. Voss[30], J. H. Vossebeld[74], N. Vranjes[13], M. Vranjes Milosavljevic[13], V. Vrba[127], M. Vreeswijk[107], R. Vuillermet[30], I. Vukotic[31], Z. Vykydal[128], P. Wagner[21], W. Wagner[175], H. Wahlberg[71], S. Wahrmund[44], J. Wakabayashi[103], J. Walder[72], R. Walker[100], W. Walkowiak[141], C. Wang[151], F. Wang[173], H. Wang[15], H. Wang[40], J. Wang[42], J. Wang[33a], K. Wang[87], R. Wang[6], S. M. Wang[151], T. Wang[21], T. Wang[35], X. Wang[176], C. Wanotayaroj[116], A. Warburton[87], C. P. Ward[28], D. R. Wardrope[78], A. Washbrook[46], C. Wasicki[42], P. M. Watkins[18], A. T. Watson[18], I. J. Watson[150], M. F. Watson[18], G. Watts[138], S. Watts[84], B. M. Waugh[78], S. Webb[84], M. S. Weber[17], S. W. Weber[174], J. S. Webster[31], A. R. Weidberg[120], B. Weinert[61], J. Weingarten[54], C. Weiser[48], H. Weits[107], P. S. Wells[30], T. Wenaus[25], T. Wengler[30], S. Wenig[30], N. Wermes[21], M. Werner[48], P. Werner[30], M. Wessels[58a], J. Wetter[161], K. Whalen[116], A. M. Wharton[72], A. White[8], M. J. White[1], R. White[32b], S. White[124a,124b], D. Whiteson[163], F. J. Wickens[131], W. Wiedenmann[173], M. Wielers[131], P. Wienemann[21], C. Wiglesworth[36], L. A. M. Wiik-Fuchs[21], A. Wildauer[101], H. G. Wilkens[30], H. H. Williams[122], S. Williams[107], C. Willis[90], S. Willocq[86], A. Wilson[89], J. A. Wilson[18], I. Wingerter-Seez[5], F. Winklmeier[116], B. T. Winter[21], M. Wittgen[143], J. Wittkowski[100], S. J. Wollstadt[83], M. W. Wolter[39], H. Wolters[126a,126c], B. K. Wosiek[39], J. Wotschack[30], M. J. Woudstra[84], K. W. Wozniak[39], M. Wu[55], M. Wu[31], S. L. Wu[173], X. Wu[49], Y. Wu[89], T. R. Wyatt[84], B. M. Wynne[46], S. Xella[36], D. Xu[33a], L. Xu[25], B. Yabsley[150], S. Yacoob[145a], R. Yakabe[67], M. Yamada[66], D. Yamaguchi[157], Y. Yamaguchi[118], A. Yamamoto[66], S. Yamamoto[155], T. Yamanaka[155], K. Yamauchi[103], Y. Yamazaki[67], Z. Yan[22], H. Yang[33e], H. Yang[173], Y. Yang[151], W-M. Yao[15], Y. Yasu[66], E. Yatsenko[5], K. H. Yau Wong[21], J. Ye[40], S. Ye[25], I. Yeletskikh[65], A. L. Yen[57], E. Yildirim[42], K. Yorita[171], R. Yoshida[6], K. Yoshihara[122], C. Young[143], C. J. S. Young[30], S. Youssef[22], D. R. Yu[15], J. Yu[8], J. M. Yu[89], J. Yu[114], L. Yuan[67], S. P. Y. Yuen[21], A. Yurkewicz[108], I. Yusuff[28,ak], B. Zabinski[39], R. Zaidan[63], A. M. Zaitsev[130,ab], J. Zalieckas[14], A. Zaman[148], S. Zambito[57], L. Zanello[132a,132b], D. Zanzi[88], C. Zeitnitz[175], M. Zeman[128], A. Zemla[38a], Q. Zeng[143], K. Zengel[23], O. Zenin[130], T. Ženiš[144a], D. Zerwas[117], D. Zhang[89], F. Zhang[173], H. Zhang[33c], J. Zhang[6], L. Zhang[48], R. Zhang[33b,i], X. Zhang[33d], Z. Zhang[117], X. Zhao[40], Y. Zhao[33d,117], Z. Zhao[33b], A. Zhemchugov[65], J. Zhong[120], B. Zhou[89], C. Zhou[45], L. Zhou[35], L. Zhou[40], M. Zhou[148], N. Zhou[33f], C. G. Zhu[33d], H. Zhu[33a], J. Zhu[89], Y. Zhu[33b], X. Zhuang[33a], K. Zhukov[96], A. Zibell[174], D. Zieminska[61], N. I. Zimine[65], C. Zimmermann[83], S. Zimmermann[48], Z. Zinonos[54], M. Zinser[83], M. Ziolkowski[141], L. Živković[13], G. Zobernig[173], A. Zoccoli[20a,20b], M. zur Nedden[16], G. Zurzolo[104a,104b], L. Zwalinski[30]

[1] Department of Physics, University of Adelaide, Adelaide, Australia
[2] Physics Department, SUNY Albany, Albany, NY, USA
[3] Department of Physics, University of Alberta, Edmonton, AB, Canada
[4] [(a)]Department of Physics, Ankara University, Ankara, Turkey; [(b)]Istanbul Aydin University, Istanbul, Turkey; [(c)]Division of Physics, TOBB University of Economics and Technology, Ankara, Turkey
[5] LAPP, CNRS/IN2P3 and Université Savoie Mont Blanc, Annecy-le-Vieux, France
[6] High Energy Physics Division, Argonne National Laboratory, Argonne, IL, USA
[7] Department of Physics, University of Arizona, Tucson, AZ, USA
[8] Department of Physics, The University of Texas at Arlington, Arlington, TX, USA
[9] Physics Department, University of Athens, Athens, Greece
[10] Physics Department, National Technical University of Athens, Zografou, Greece
[11] Institute of Physics, Azerbaijan Academy of Sciences, Baku, Azerbaijan
[12] Institut de Física d'Altes Energies and Departament de Física de la Universitat Autònoma de Barcelona, Barcelona, Spain
[13] Institute of Physics, University of Belgrade, Belgrade, Serbia
[14] Department for Physics and Technology, University of Bergen, Bergen, Norway
[15] Physics Division, Lawrence Berkeley National Laboratory and University of California, Berkeley, CA, USA
[16] Department of Physics, Humboldt University, Berlin, Germany
[17] Albert Einstein Center for Fundamental Physics and Laboratory for High Energy Physics, University of Bern, Bern, Switzerland
[18] School of Physics and Astronomy, University of Birmingham, Birmingham, UK
[19] [(a)]Department of Physics, Bogazici University, Istanbul, Turkey; [(b)]Department of Physics Engineering, Gaziantep University, Gaziantep, Turkey; [(c)]Department of Physics, Dogus University, Istanbul, Turkey

[20] [a]INFN Sezione di Bologna, Bologna, Italy; [b]Dipartimento di Fisica e Astronomia, Università di Bologna, Bologna, Italy
[21] Physikalisches Institut, University of Bonn, Bonn, Germany
[22] Department of Physics, Boston University, Boston, MA, USA
[23] Department of Physics, Brandeis University, Waltham, MA, USA
[24] [a]Universidade Federal do Rio De Janeiro COPPE/EE/IF, Rio de Janeiro, Brazil; [b]Electrical Circuits Department, Federal University of Juiz de Fora (UFJF), Juiz de Fora, Brazil; [c]Federal University of Sao Joao del Rei (UFSJ), Sao Joao del Rei, Brazil; [d]Instituto de Fisica, Universidade de Sao Paulo, Sao Paulo, Brazil
[25] Physics Department, Brookhaven National Laboratory, Upton, NY, USA
[26] [a]National Institute of Physics and Nuclear Engineering, Bucharest, Romania; [b]Physics Department, National Institute for Research and Development of Isotopic and Molecular Technologies, Cluj Napoca, Romania; [c]University Politehnica Bucharest, Bucharest, Romania; [d]West University in Timisoara, Timisoara, Romania
[27] Departamento de Física, Universidad de Buenos Aires, Buenos Aires, Argentina
[28] Cavendish Laboratory, University of Cambridge, Cambridge, UK
[29] Department of Physics, Carleton University, Ottawa, ON, Canada
[30] CERN, Geneva, Switzerland
[31] Enrico Fermi Institute, University of Chicago, Chicago, IL, USA
[32] [a]Departamento de Física, Pontificia Universidad Católica de Chile, Santiago, Chile; [b]Departamento de Física, Universidad Técnica Federico Santa María, Valparaiso, Chile
[33] [a]Institute of High Energy Physics, Chinese Academy of Sciences, Beijing, China; [b]Department of Modern Physics, University of Science and Technology of China, Hefei, Anhui, China; [c]Department of Physics, Nanjing University, Jiangsu, China; [d]School of Physics, Shandong University, Shandong, China; [e]Shanghai Key Laboratory for Particle Physics and Cosmology, Department of Physics and Astronomy, Shanghai Jiao Tong University, Shanghai, China ; [f]Physics Department, Tsinghua University, Beijing 100084, China
[34] Laboratoire de Physique Corpusculaire, Clermont Université and Université Blaise Pascal and CNRS/IN2P3, Clermont-Ferrand, France
[35] Nevis Laboratory, Columbia University, Irvington, NY, USA
[36] Niels Bohr Institute, University of Copenhagen, Copenhagen, Denmark
[37] [a]INFN Gruppo Collegato di Cosenza, Laboratori Nazionali di Frascati, Frascati, Italy; [b]Dipartimento di Fisica, Università della Calabria, Rende, Italy
[38] [a]AGH University of Science and Technology, Faculty of Physics and Applied Computer Science, Krakow, Poland; [b]Marian Smoluchowski Institute of Physics, Jagiellonian University, Krakow, Poland
[39] Institute of Nuclear Physics, Polish Academy of Sciences, Krakow, Poland
[40] Physics Department, Southern Methodist University, Dallas, TX, USA
[41] Physics Department, University of Texas at Dallas, Richardson, TX, USA
[42] DESY, Hamburg and Zeuthen, Germany
[43] Institut für Experimentelle Physik IV, Technische Universität Dortmund, Dortmund, Germany
[44] Institut für Kern- und Teilchenphysik, Technische Universität Dresden, Dresden, Germany
[45] Department of Physics, Duke University, Durham, NC, USA
[46] SUPA-School of Physics and Astronomy, University of Edinburgh, Edinburgh, UK
[47] INFN Laboratori Nazionali di Frascati, Frascati, Italy
[48] Fakultät für Mathematik und Physik, Albert-Ludwigs-Universität, Freiburg, Germany
[49] Section de Physique, Université de Genève, Geneva, Switzerland
[50] [a]INFN Sezione di Genova, Genoa, Italy; [b]Dipartimento di Fisica, Università di Genova, Genoa, Italy
[51] [a]E. Andronikashvili Institute of Physics, Iv. Javakhishvili Tbilisi State University, Tbilisi, Georgia; [b]High Energy Physics Institute, Tbilisi State University, Tbilisi, Georgia
[52] II Physikalisches Institut, Justus-Liebig-Universität Giessen, Giessen, Germany
[53] SUPA-School of Physics and Astronomy, University of Glasgow, Glasgow, UK
[54] II Physikalisches Institut, Georg-August-Universität, Göttingen, Germany
[55] Laboratoire de Physique Subatomique et de Cosmologie, Université Grenoble-Alpes, CNRS/IN2P3, Grenoble, France
[56] Department of Physics, Hampton University, Hampton, VA, USA
[57] Laboratory for Particle Physics and Cosmology, Harvard University, Cambridge, MA, USA

[58] [(a)]Kirchhoff-Institut für Physik, Ruprecht-Karls-Universität Heidelberg, Heidelberg, Germany; [(b)]Physikalisches Institut, Ruprecht-Karls-Universität Heidelberg, Heidelberg, Germany; [(c)]ZITI Institut für technische Informatik, Ruprecht-Karls-Universität Heidelberg, Mannheim, Germany
[59] Faculty of Applied Information Science, Hiroshima Institute of Technology, Hiroshima, Japan
[60] [(a)]Department of Physics, The Chinese University of Hong Kong, Shatin, NT, Hong Kong; [(b)]Department of Physics, The University of Hong Kong, Pokfulam, Hong Kong; [(c)]Department of Physics, The Hong Kong University of Science and Technology, Clear Water Bay, Kowloon, Hong Kong, China
[61] Department of Physics, Indiana University, Bloomington, IN, USA
[62] Institut für Astro- und Teilchenphysik, Leopold-Franzens-Universität, Innsbruck, Austria
[63] University of Iowa, Iowa City, IA, USA
[64] Department of Physics and Astronomy, Iowa State University, Ames, IA, USA
[65] Joint Institute for Nuclear Research, JINR Dubna, Dubna, Russia
[66] KEK, High Energy Accelerator Research Organization, Tsukuba, Japan
[67] Graduate School of Science, Kobe University, Kobe, Japan
[68] Faculty of Science, Kyoto University, Kyoto, Japan
[69] Kyoto University of Education, Kyoto, Japan
[70] Department of Physics, Kyushu University, Fukuoka, Japan
[71] Instituto de Física La Plata, Universidad Nacional de La Plata and CONICET, La Plata, Argentina
[72] Physics Department, Lancaster University, Lancaster, UK
[73] [(a)]INFN Sezione di Lecce, Lecce, Italy; [(b)]Dipartimento di Matematica e Fisica, Università del Salento, Lecce, Italy
[74] Oliver Lodge Laboratory, University of Liverpool, Liverpool, UK
[75] Department of Physics, Jožef Stefan Institute and University of Ljubljana, Ljubljana, Slovenia
[76] School of Physics and Astronomy, Queen Mary University of London, London, UK
[77] Department of Physics, Royal Holloway University of London, Surrey, UK
[78] Department of Physics and Astronomy, University College London, London, UK
[79] Louisiana Tech University, Ruston, LA, USA
[80] Laboratoire de Physique Nucléaire et de Hautes Energies, UPMC and Université Paris-Diderot and CNRS/IN2P3, Paris, France
[81] Fysiska institutionen, Lunds universitet, Lund, Sweden
[82] Departamento de Fisica Teorica C-15, Universidad Autonoma de Madrid, Madrid, Spain
[83] Institut für Physik, Universität Mainz, Mainz, Germany
[84] School of Physics and Astronomy, University of Manchester, Manchester, UK
[85] CPPM, Aix-Marseille Université and CNRS/IN2P3, Marseille, France
[86] Department of Physics, University of Massachusetts, Amherst, MA, USA
[87] Department of Physics, McGill University, Montreal, QC, Canada
[88] School of Physics, University of Melbourne, Melbourne, VIC, Australia
[89] Department of Physics, The University of Michigan, Ann Arbor, MI, USA
[90] Department of Physics and Astronomy, Michigan State University, East Lansing, MI, USA
[91] [(a)]INFN Sezione di Milano, Milan, Italy; [(b)]Dipartimento di Fisica, Università di Milano, Milan, Italy
[92] B.I. Stepanov Institute of Physics, National Academy of Sciences of Belarus, Minsk, Republic of Belarus
[93] National Scientific and Educational Centre for Particle and High Energy Physics, Minsk, Republic of Belarus
[94] Department of Physics, Massachusetts Institute of Technology, Cambridge, MA, USA
[95] Group of Particle Physics, University of Montreal, Montreal, QC, Canada
[96] P.N. Lebedev Institute of Physics, Academy of Sciences, Moscow, Russia
[97] Institute for Theoretical and Experimental Physics (ITEP), Moscow, Russia
[98] National Research Nuclear University MEPhI, Moscow, Russia
[99] D.V. Skobeltsyn Institute of Nuclear Physics, M.V. Lomonosov Moscow State University, Moscow, Russia
[100] Fakultät für Physik, Ludwig-Maximilians-Universität München, Munich, Germany
[101] Max-Planck-Institut für Physik (Werner-Heisenberg-Institut), München, Germany
[102] Nagasaki Institute of Applied Science, Nagasaki, Japan
[103] Graduate School of Science and Kobayashi-Maskawa Institute, Nagoya University, Nagoya, Japan
[104] [(a)]INFN Sezione di Napoli, Naples, Italy; [(b)]Dipartimento di Fisica, Università di Napoli, Naples, Italy
[105] Department of Physics and Astronomy, University of New Mexico, Albuquerque, NM, USA

[106] Institute for Mathematics, Astrophysics and Particle Physics, Radboud University Nijmegen/Nikhef, Nijmegen, The Netherlands
[107] Nikhef National Institute for Subatomic Physics and University of Amsterdam, Amsterdam, The Netherlands
[108] Department of Physics, Northern Illinois University, De Kalb, IL, USA
[109] Budker Institute of Nuclear Physics, SB RAS, Novosibirsk, Russia
[110] Department of Physics, New York University, New York, NY, USA
[111] Ohio State University, Columbus, OH, USA
[112] Faculty of Science, Okayama University, Okayama, Japan
[113] Homer L. Dodge Department of Physics and Astronomy, University of Oklahoma, Norman, OK, USA
[114] Department of Physics, Oklahoma State University, Stillwater, OK, USA
[115] Palacký University, RCPTM, Olomouc, Czech Republic
[116] Center for High Energy Physics, University of Oregon, Eugene, OR, USA
[117] LAL, Université Paris-Sud and CNRS/IN2P3, Orsay, France
[118] Graduate School of Science, Osaka University, Osaka, Japan
[119] Department of Physics, University of Oslo, Oslo, Norway
[120] Department of Physics, Oxford University, Oxford, UK
[121] [(a)]INFN Sezione di Pavia, Pavia, Italy; [(b)]Dipartimento di Fisica, Università di Pavia, Pavia, Italy
[122] Department of Physics, University of Pennsylvania, Philadelphia, PA, USA
[123] National Research Centre "Kurchatov Institute" B.P.Konstantinov Petersburg Nuclear Physics Institute, St. Petersburg, Russia
[124] [(a)]INFN Sezione di Pisa, Pisa, Italy; [(b)]Dipartimento di Fisica E. Fermi, Università di Pisa, Pisa, Italy
[125] Department of Physics and Astronomy, University of Pittsburgh, Pittsburgh, PA, USA
[126] [(a)]Laboratório de Instrumentação e Física Experimental de Partículas-LIP, Lisbon, Portugal; [(b)]Faculdade de Ciências, Universidade de Lisboa, Lisbon, Portugal; [(c)]Department of Physics, University of Coimbra, Coimbra, Portugal; [(d)]Centro de Física Nuclear da Universidade de Lisboa, Lisbon, Portugal; [(e)]Departamento de Fisica, Universidade do Minho, Braga, Portugal; [(f)]Departamento de Fisica Teorica y del Cosmos and CAFPE, Universidad de Granada, Granada, Spain ; [(g)]Dep Fisica and CEFITEC of Faculdade de Ciencias e Tecnologia, Universidade Nova de Lisboa, Caparica, Portugal
[127] Institute of Physics, Academy of Sciences of the Czech Republic, Prague, Czech Republic
[128] Czech Technical University in Prague, Prague, Czech Republic
[129] Faculty of Mathematics and Physics, Charles University in Prague, Prague, Czech Republic
[130] State Research Center Institute for High Energy Physics, Protvino, Russia
[131] Particle Physics Department, Rutherford Appleton Laboratory, Didcot, UK
[132] [(a)]INFN Sezione di Roma, Rome, Italy; [(b)]Dipartimento di Fisica, Sapienza Università di Roma, Rome, Italy
[133] [(a)]INFN Sezione di Roma Tor Vergata, Rome, Italy; [(b)]Dipartimento di Fisica, Università di Roma Tor Vergata, Rome, Italy
[134] [(a)]INFN Sezione di Roma Tre, Rome, Italy; [(b)]Dipartimento di Matematica e Fisica, Università Roma Tre, Rome, Italy
[135] [(a)]Faculté des Sciences Ain Chock, Réseau Universitaire de Physique des Hautes Energies-Université Hassan II, Casablanca, Morocco; [(b)]Centre National de l'Energie des Sciences Techniques Nucleaires, Rabat, Morocco; [(c)]Faculté des Sciences Semlalia, Université Cadi Ayyad, LPHEA-Marrakech, Marrakech, Morocco; [(d)]Faculté des Sciences, Université Mohamed Premier and LPTPM, Oujda, Morocco; [(e)]Faculté des Sciences, Université Mohammed V, Rabat, Morocco
[136] DSM/IRFU (Institut de Recherches sur les Lois Fondamentales de l'Univers), CEA Saclay (Commissariat à l'Energie Atomique et aux Energies Alternatives), Gif-sur-Yvette, France
[137] Santa Cruz Institute for Particle Physics, University of California Santa Cruz, Santa Cruz, CA, USA
[138] Department of Physics, University of Washington, Seattle, WA, USA
[139] Department of Physics and Astronomy, University of Sheffield, Sheffield, UK
[140] Department of Physics, Shinshu University, Nagano, Japan
[141] Fachbereich Physik, Universität Siegen, Siegen, Germany
[142] Department of Physics, Simon Fraser University, Burnaby, BC, Canada
[143] SLAC National Accelerator Laboratory, Stanford, CA, USA
[144] [(a)]Faculty of Mathematics, Physics and Informatics, Comenius University, Bratislava, Slovak Republic; [(b)]Department of Subnuclear Physics, Institute of Experimental Physics of the Slovak Academy of Sciences, Kosice, Slovak Republic

[145] [(a)]Department of Physics, University of Cape Town, Cape Town, South Africa; [(b)]Department of Physics, University of Johannesburg, Johannesburg, South Africa; [(c)]School of Physics, University of the Witwatersrand, Johannesburg, South Africa
[146] [(a)]Department of Physics, Stockholm University, Stockholm, Sweden; [(b)]The Oskar Klein Centre, Stockholm, Sweden
[147] Physics Department, Royal Institute of Technology, Stockholm, Sweden
[148] Departments of Physics and Astronomy and Chemistry, Stony Brook University, Stony Brook, NY, USA
[149] Department of Physics and Astronomy, University of Sussex, Brighton, UK
[150] School of Physics, University of Sydney, Sydney, Australia
[151] Institute of Physics, Academia Sinica, Taipei, Taiwan
[152] Department of Physics, Technion: Israel Institute of Technology, Haifa, Israel
[153] Raymond and Beverly Sackler School of Physics and Astronomy, Tel Aviv University, Tel Aviv, Israel
[154] Department of Physics, Aristotle University of Thessaloniki, Thessaloníki, Greece
[155] International Center for Elementary Particle Physics and Department of Physics, The University of Tokyo, Tokyo, Japan
[156] Graduate School of Science and Technology, Tokyo Metropolitan University, Tokyo, Japan
[157] Department of Physics, Tokyo Institute of Technology, Tokyo, Japan
[158] Department of Physics, University of Toronto, Toronto, ON, Canada
[159] [(a)]TRIUMF, Vancouver, BC, Canada; [(b)]Department of Physics and Astronomy, York University, Toronto, ON, Canada
[160] Faculty of Pure and Applied Sciences, University of Tsukuba, Tsukuba, Japan
[161] Department of Physics and Astronomy, Tufts University, Medford, MA, USA
[162] Centro de Investigaciones, Universidad Antonio Narino, Bogotá, Colombia
[163] Department of Physics and Astronomy, University of California Irvine, Irvine, CA, USA
[164] [(a)]INFN Gruppo Collegato di Udine, Sezione di Trieste, Udine, Italy; [(b)]ICTP, Trieste, Italy; [(c)]Dipartimento di Chimica Fisica e Ambiente, Università di Udine, Udine, Italy
[165] Department of Physics, University of Illinois, Urbana, IL, USA
[166] Department of Physics and Astronomy, University of Uppsala, Uppsala, Sweden
[167] Instituto de Física Corpuscular (IFIC) and Departamento de Física Atómica, Molecular y Nuclear and Departamento de Ingeniería Electrónica and Instituto de Microelectrónica de Barcelona (IMB-CNM), University of Valencia and CSIC, Valencia, Spain
[168] Department of Physics, University of British Columbia, Vancouver, BC, Canada
[169] Department of Physics and Astronomy, University of Victoria, Victoria, BC, Canada
[170] Department of Physics, University of Warwick, Coventry, UK
[171] Waseda University, Tokyo, Japan
[172] Department of Particle Physics, The Weizmann Institute of Science, Rehovot, Israel
[173] Department of Physics, University of Wisconsin, Madison, WI, USA
[174] Fakultät für Physik und Astronomie, Julius-Maximilians-Universität, Würzburg, Germany
[175] Fachbereich C Physik, Bergische Universität Wuppertal, Wuppertal, Germany
[176] Department of Physics, Yale University, New Haven, CT, USA
[177] Yerevan Physics Institute, Yerevan, Armenia
[178] Centre de Calcul de l'Institut National de Physique Nucléaire et de Physique des Particules (IN2P3), Villeurbanne, France

[a] Also at Department of Physics, King's College London, London, UK
[b] Also at Institute of Physics, Azerbaijan Academy of Sciences, Baku, Azerbaijan
[c] Also at Novosibirsk State University, Novosibirsk, Russia
[d] Also at TRIUMF, Vancouver, BC, Canada
[e] Also at Department of Physics, California State University, Fresno, CA, USA
[f] Also at Department of Physics, University of Fribourg, Fribourg, Switzerland
[g] Also at Departamento de Fisica e Astronomia, Faculdade de Ciencias, Universidade do Porto, Porto, Portugal
[h] Also at Tomsk State University, Tomsk, Russia
[i] Also at CPPM, Aix-Marseille Université and CNRS/IN2P3, Marseille, France
[j] Also at Universita di Napoli Parthenope, Napoli, Italy
[k] Also at Institute of Particle Physics (IPP), Canada
[l] Also at Particle Physics Department, Rutherford Appleton Laboratory, Didcot, UK
[m] Also at Department of Physics, St. Petersburg State Polytechnical University, St. Petersburg, Russia

[n] Also at Louisiana Tech University, Ruston, LA, USA
[o] Also at Institucio Catalana de Recerca i Estudis Avancats, ICREA, Barcelona, Spain
[p] Also at Graduate School of Science, Osaka University, Osaka, Japan
[q] Also at Department of Physics, National Tsing Hua University, Taiwan
[r] Also at Department of Physics, The University of Texas at Austin, Austin, TX, USA
[s] Also at Institute of Theoretical Physics, Ilia State University, Tbilisi, Georgia
[t] Also at CERN, Geneva, Switzerland
[u] Also at Georgian Technical University (GTU), Tbilisi, Georgia
[v] Also at Manhattan College, New York, NY, USA
[w] Also at Hellenic Open University, Patras, Greece
[x] Also at Institute of Physics, Academia Sinica, Taipei, Taiwan
[y] Also at LAL, Université Paris-Sud and CNRS/IN2P3, Orsay, France
[z] Also at Academia Sinica Grid Computing, Institute of Physics, Academia Sinica, Taipei, Taiwan
[aa] Also at School of Physics, Shandong University, Shandong, China
[ab] Also at Moscow Institute of Physics and Technology State University, Dolgoprudny, Russia
[ac] Also at Section de Physique, Université de Genève, Geneva, Switzerland
[ad] Also at International School for Advanced Studies (SISSA), Trieste, Italy
[ae] Also at Department of Physics and Astronomy, University of South Carolina, Columbia, SC, USA
[af] Also at School of Physics and Engineering, Sun Yat-sen University, Guangzhou, China
[ag] Also at Faculty of Physics, M.V.Lomonosov Moscow State University, Moscow, Russia
[ah] Also at National Research Nuclear University MEPhI, Moscow, Russia
[ai] Also at Department of Physics, Stanford University, Stanford CA, USA
[aj] Also at Institute for Particle and Nuclear Physics, Wigner Research Centre for Physics, Budapest, Hungary
[ak] Also at University of Malaya, Department of Physics, Kuala Lumpur, Malaysia
* Deceased